Electronic Supplementary Information for

Slip to π Ru: Structural distortions due to metal-iminoxolene π bonding

Patricia Rose H. Ayson and Seth N. Brown*
251 Nieuwland Science Hall, Department of Chemistry and Biochemistry
University of Notre Dame, Notre Dame, IN 46556-5670 USA

Table of Contents

I. Procedures and preparative details

General Procedures. Except as noted, all procedures were carried out in an inert-atmosphere glovebox. Deuterated solvents were obtained from Cambridge Isotope Labs. CD_2Cl_2 and $CDCl_3$ were dried over 4 Å molecular sieves, followed by CaH_2, and were stored in the drybox before use. CF_2Cl_2 was purchased from SynQuest Laboratories Inc. $CDFCl_2$ was prepared by the literature method.[S1] Dry protio solvents were purchased as anhydrous grade and stored in the drybox before use. Di-μ-chlorobis[(*p*-cymene)chlororuthenium(II)] was purchased from Strem Chemicals or from TCI Chemicals and used as received, while the analogous osmium complex was prepared from H_2OsCl_6 and α-terpinene.[S2] Diso (*N*-(2,6-diisopropylphenyl)-4,6-di-*tert*-butyl-2-imino-*o*-benzoquinone)[S3] and 3,5,3",5"-tetrakis(trifluoromethyl)-2'-amino-*m*-terphenyl[S4] were prepared as described in the literature. ^1H and $^{13}C\{^1H\}$ NMR spectra were measured using a Bruker Avance DPX-400 or -500 spectrometer and were referenced to the solvent residual signals. $^{19}F\{^1H\}$ NMR spectra were referenced to $CFCl_3$ while $^{31}P\{^1H\}$ NMR spectra were referenced to external 85% H_3PO_4. Infrared spectra were recorded on a JASCO FT/IR-6300 spectrometer. UV-visible spectra were measured in a 1-cm quartz cell on a Thermo Scientific Evolution Array spectrophotometer. Elemental analyses were performed by Midwest Microanalytical Laboratories (Indianapolis, IN, USA) or by Robertson Microlit Inc (Ledgewood, NJ, USA).

***Cis*- and *trans*-dichlorobis(*N*-(2,6-diisopropylphenyl)-3,5-di-*tert*-butyl-1,2-benzoiminoxolene)ruthenium, $(Diso)_2RuCl_2$.** A mixture of 238.8 mg $\{(p\text{-cymene})RuCl_2\}_2$ (0.780 mmol Ru) and 992.3 mg Diso (2.614 mmol, 3.4 equiv) is dissolved in 12 mL dry $CHCl_3$ in the glovebox. The mixture is placed in a 20 mL scintillation vial with a stirbar, sealed, and heated in a 74 °C oil bath for 2 d. The vial is then opened to the air and the volatiles removed on

a rotary evaporator. The residue is treated with 5 mL hexane and, after standing 10 min, the hexane is decanted away from the solid, which is then washed with 3 mL additional hexane, which is combined with the first extract. The hexane extract is allowed to stand at room temperature overnight to yield a second crop of crude solid. The first crop of solid is mostly the purple *cis* isomer (R_f = 0.50, CH_2Cl_2), while the second crop is mostly the *trans* isomer (R_f = 0.80, CH_2Cl_2). The two crops of solid are dissolved in CH_2Cl_2 and eluted (separately) through short silica gel columns with dichloromethane. The green and purple bands are collected in fractions, which are checked for purity by TLC; any fractions containing a mixture of the two isomers are rechromatographed. The solvent is evaporated from the two purified isomers. The slower-moving purple material is then slurried in 3 mL CH_3CN, suction filtered, washed with 3 mL CH_3CN, and air-dried 30 min to give 0.2143 g ***cis*-(Diso)$_2$RuCl$_2$** (30%). ^{1}H NMR ($CDCl_3$): δ 0.93 (d, 6.6 Hz, 6H, CH(C*H*$_3$)$_2$), 0.95 (d, 6.6 Hz, 6H, CH(C*H*$_3$)$_2$), 1.18 (s, 18H, ^{t}Bu), 1.19 (d, 6.6 Hz, 6H, CH(C*H*$_3$)$_2$), 1.25 (s, 18H, ^{t}Bu), 1.27 (d, 6.8 Hz, 6H, CH(C*H*$_3$)$_2$), 2.86 (sept, 6.6 Hz, 2H, C*H*(CH$_3$)$_2$), 3.09 (sept, 6.6 Hz, 2H, C*H*(CH$_3$)$_2$), 6.82 (d, 2.0 Hz, 2H, iminoxolene 3- or 5-H), 7.26 (dd, 7.7, 1.3 Hz, 2H, Ar 3- or 5-H), 7.28 (dd, 7.5, 1.3 Hz, 2H, Ar 3- or 5-H), 7.42 (t, 7.7 Hz, 2H, Ar 4-H), 7.84 (d, 2.0 Hz, iminoxolene 3- or 5-H). ^{13}C{^{1}H} NMR ($CDCl_3$): δ 24.07 (CH(*C*H$_3$)$_2$), 24.71 (CH(*C*H$_3$)$_2$), 24.82 (CH(*C*H$_3$)$_2$), 26.29 (CH(*C*H$_3$)$_2$), 28.47 (*C*H(CH$_3$)$_2$), 28.62 (*C*H(CH$_3$)$_2$), 29.63 (C(*C*H$_3$)$_3$), 30.35 (C(*C*H$_3$)$_3$), 35.34 (*C*(CH$_3$)$_3$), 35.42 (*C*(CH$_3$)$_3$), 115.14, 123.27, 124.94, 127.65, 128.69, 140.95, 141.04, 144.73, 147.05, 150.42, 163.64, 185.25 (*C*O). IR (ATR, cm^{-1}): 3062 (w), 2965 (m), 2864 (m), 1590 (w), 1519 (m), 1463 (m), 1398 (w), 1377 (m), 1359 (s), 1327 (w), 1291 (s), 1257 (s), 1240 (s), 1206 (m), 1158 (m), 1100 (m), 1056 (w), 1029 (m), 993 (m), 935 (w), 904 (m), 872 (m), 825 (w), 797 (s), 784 (w), 767 (w), 740 (s). UV-

Vis-NIR (CH_2Cl_2): λ_{max} = 747 nm (ε = 10500 L mol^{-1} cm^{-1}), 566 (4460), 330 (4200). Anal. Calcd for $C_{52}H_{74}Cl_2N_2O_2Ru$: C, 67.08; H, 8.01; N, 3.01. Found: C, 66.93; H, 7.93; N, 2.94.

The faster-eluting green fraction is slurried in hexane (3 mL), suction filtered, washed with 3 mL hexane, and air-dried 20 min to give 0.1076 g ***trans*-(Diso)$_2$RuCl$_2$** (15%). ^{1}H NMR (CD_2Cl_2): δ 0.94 (d, 6.8 Hz, 12H, CH(C*H*$_3$)$_2$), 1.09 (d, 6.6 Hz, 12H, CH(C*H*$_3$)$_2$), 1.10 (s, 18H, ^{t}Bu), 1.22 (s, 18H, ^{t}Bu), 2.71 (sept, 6.7 Hz, 4H, C*H*(CH$_3$)$_2$), 6.81 (d, 2.0 Hz, 2H, iminoxolene 3- or 5-H), 7.12 (d, 7.8 Hz, 4H, Ar 3,5-H), 7.42 (t, 7.8 Hz, 2H, Ar 4-H), 7.94 (d, 2.0 Hz, 2H, iminoxolene 3- or 5-H). ^{13}C{^{1}H} NMR (CD_2Cl_2): δ 24.34 (CH(*C*H$_3$)$_2$), 25.48 (CH(*C*H$_3$)$_2$), 28.79 (C(*C*H$_3$)$_3$), 28.89 (*C*H(CH$_3$)$_2$), 30.46 (C(*C*H$_3$)$_3$), 35.35 (*C*(CH$_3$)$_3$), 36.14 (*C*(CH$_3$)$_3$), 115.48, 124.63 (Ar 3,5-*C*), 125.52, 128.75, 140.17, 148.46, 148.90, 150.49, 168.90, 183.26 (*C*O). IR (ATR, cm^{-1}): 3086 (w), 3063 (w), 2960 (s), 2927 (w), 2906 (w), 2865 (w), 1598 (w), 1523 (m), 1480 (m), 1465 (m), 1396 (w), 1356 (s), 1327 (w), 1297 (s), 1265 (s), 1252 (m), 1240 (m), 1207 (w), 1160 (s) 1105 (m), 1096 (m), 1057 (w), 1042 (w), 1026 (m), 993 (m), 953 (w), 933 (w), 913 (m), 906 (m), 876 (w), 867 (w), 825 (w), 796 (m), 791 (w), 778 (w), 767 (w), 740 (m), 712 (w), 692 (w), 674 (w), 661 (w). UV-Vis-NIR (CH_2Cl_2): λ_{max} = 962 nm (ε = 4800 L mol^{-1} cm^{-1}), 743 (16000), 523 (sh, 3600), 455 (sh, 4600), 355 (7100). Anal. Calcd for $C_{52}H_{74}Cl_2N_2O_2Ru$: C, 67.08; H, 8.01; N, 3.01. Found: C, 66.79; H, 7.88; N, 3.07.

***Cis*- and *trans*-dichlorobis(*N*-(2,6-diisopropylphenyl)-3,5-di-*tert*-butyl-1,2-benzoiminoxolene)osmium, (Diso)$_2$OsCl$_2$.** To a glass bomb are added 1.0 g {(*p*-cymene)$OsCl_2$}$_2$ (2.5 mmol Os), 3.79 g Diso (9.98 mmol, 3.9 equiv), 70 mL $CHCl_3$, and a stirbar. The bomb is sealed with a Teflon valve and taken out of the glovebox and heated with stirring in a 75 °C oil bath. After 1 d, the bomb is opened to the air and the reaction mixture transferred to a round-bottom flask. The solvent is evaporated using a rotary evaporator. The

purple residue is dissolved in 60:40 cyclohexane:CH_2Cl_2 and eluted through a silica gel column using this solvent mixture. The fast-moving green fraction containing the *trans* isomer is collected, then the eluent is changed to 100% CH_2Cl_2 to elute the *cis* isomer as a purple band. The purple fraction is evaporated using the rotary evaporator and the residue slurried in 7 mL of hexanes. After 1 h, the purple crystals are collected through a frit by vacuum filtration to give 162.1 mg of ***cis*-(Diso)$_2$OsCl$_2$** (5%). ^{1}H NMR (CD_2Cl_2): δ 0.85 (d, 6.8 Hz, 6H, CH(CH_3)$_2$), 1.10 (d, 6.7 Hz, 6H, CH(CH_3)$_2$), 1.23 (s, 18H, ^{t}Bu), 1.29 (d, 6.6 Hz, 6H, CH(CH_3)$_2$), 1.34 (s, 18H, ^{t}Bu), 1.39 (d, 6.6 Hz, 6H, CH(CH_3)$_2$), 2.55 (sept, 6.7 Hz, 2H, CH(CH$_3$)$_2$), 2.59 (sept, 6.7 Hz, 2H, CH(CH$_3$)$_2$), 3.87 (d, 1.7 Hz, 2H, iminoxolene 3- or 5-H), 4.78 (d, 1.8 Hz, iminoxolene 3- or 5-H), 7.44 (t, 7.7 Hz, 2H, Ar 4-H), 7.87 (d, 7.7 Hz, 2H, Ar 3- or 5-H), 8.09 (d, 7.7 Hz, 2H, Ar 3- or 5-H). ^{13}C{^{1}H} NMR (CD_2Cl_2): δ 24.42 (2C, CH(*C*H$_3$)$_2$), 25.23, 26.11, 27.89, 28.00, 28.23 (C(*C*H$_3$)$_3$), 31.82 (*C*(CH$_3$)$_3$), 33.20 (C(*C*H$_3$)$_3$), 35.65 (*C*(CH$_3$)$_3$), 109.17, 124.21, 126.59, 127.07, 128.85, 129.10, 136.65, 139.87, 144.98, 157.31, 160.38, 186.60 (*C*O). IR (evapd film, cm^{-1}): 3061 (w), 2965 (s), 2926 (m), 2864 (m), 1584 (w), 1544 (w), 1524 (m), 1462 (m), 1439 (w), 1395 (w), 1377 (w), 1360 (m), 1324 (w), 1317 (w), 1303 (w), 1282 (w), 1247 (m), 1231 (s), 1198 (m), 1156 (m), 1109 (w), 1055 (w), 1028 (w), 996 (w), 934 (w), 909 (w), 897 (w), 971 (w), 823 (w), 798 (w), 773 (w), 768 (w), 741 (w), 647 (w). UV-Vis (CH_2Cl_2): λ_{max} = 817 nm (sh, ε = 2300 L mol^{-1} cm^{-1}), 602 (11200), 500 (9600), 365 (sh, 3900). Anal. Calcd for $C_{52}H_{74}Cl_2N_2O_2Os$: C, 61.21; H, 7.31; N, 2.75. Found: C, 61.14; H, 7.02; N, 2.76.

The green fraction is evaporated using a rotary evaporator. The green residue is dissolved in hexanes and passed through a silica gel column. The column is eluted with hexanes to collect a yellow fraction, then the eluent is changed to 50:50 hexanes:$CHCl_3$ to collect the desired blue fraction. After evaporation of the solvent, the blue residue is crystallized from CH_2Cl_2/CH_3OH

to give 10 mg ***trans*-(Diso)$_2$OsCl$_2$** (0.4% yield). The isolated material is contaminated with a small amount of a paramagnetic impurity, as judged by ^{1}H NMR. ^{1}H NMR (CD_2Cl_2): δ 0.90 (d, 6.7 Hz, 12H, CH(CH_3)$_2$), 1.05 (d, 6.7 Hz, 12H, CH(CH_3)$_2$), 1.16 (s, 18H, ^{t}Bu), 1.37 (s, 18H, ^{t}Bu), 2.30 (sept, 7 Hz, 4H, CH(CH$_3$)$_2$), 7.07 (d, 2 Hz, 2H, iminoxolene 3- or 5-H), 7.27 (d, 8 Hz, 4H, Ar 3,5-H), 7.46 (t, 8 Hz, 2H, Ar 4-H), 7.47 (d, 2 Hz, 2H, iminoxolene 3- or 5-H).

***N*-2'-(3,5,3'',5''-tetrakis(trifluoromethyl)-*m*-terphenyl)-4,6-di-*tert*-butyl-2-iminobenzoquinone, CF$_3$Tio.** Into a 20-mL scintillation vial in the air are weighed 1.0984 g 3,5,3",5"-tetrakis(trifluoromethyl)-2'-amino-*m*-terphenyl (2.12 mmol) and 0.5019 g 3,5-di-*tert*-butyl-1,2-benzoquinone (2.28 mmol, 1.07 equiv). After adding 10 mL glacial acetic acid, the vial is securely capped with a Teflon-lined cap and the mixture shaken until everything dissolves. After standing two days at room temperature, the dark red solution is added to a round-bottom flask and the acetic acid removed on the rotary evaporator. The residue is dissolved in ~10 mL heptane and the heptane removed on the rotary evaporator (in order to remove the last traces of CH_3COOH via the heptane/acetic acid azeotrope). The residue is then dissolved in a minimum of hexane and loaded onto a plug of silica gel. The silica is eluted with 20% CH_2Cl_2/hexane, and the dark red band collected in fractions which are checked for purity by TLC. Any of the early fractions that are contaminated by faster-moving colorless impurities are combined and rerun through a plug of silica gel to remove the impurities. The pure fractions are combined and stripped down on the rotovap to give a red-brown foam, which is scraped into a vial to give 1.0386 g CF_3Tio (68%). Two isomers are observed in a 1.6 : 1 ratio in $CDCl_3$. ^{1}H NMR ($CDCl_3$): Major isomer δ 0.96 (s, 9H, ^{t}Bu), 1.17 (s, 9H, ^{t}Bu), 5.76 (d, 2.1 Hz, 1H, iminoquinone 3- or 5-H), 6.73 (d, 2.1 Hz, 1H, iminoquinone 3- or 5-H), 7.42 (t, 8.2 Hz, 1H, terphenyl 5′-H), 7.52 (d, 7.6 Hz, 2H, terphenyl 4′,6′-H), 7.75 (s, 2H, terphenyl 4,4′′-H), 7.79 (s,

4H, terphenyl 2,6,2′′,6′′-H). Minor isomer δ 0.97 (s, 9H, ^{t}Bu), 1.11 (s, 9H, ^{t}Bu), 6.30 (d, 2.0 Hz, 1H, iminoquinone 3- or 5-H), 6.75 (d, 2.2 Hz, 1H, iminoquinone 3- or 5-H), 7.33 (t, 7.6 Hz, 1H, terphenyl 5′-H), 7.45 (d, 7.5 Hz, 2H, terphenyl 4′,6′-H), 7.73 (s, 2H, terphenyl 4,4′′-H), 7.77 (s, 4H, terphenyl 2,6,2′′,6′′-H). $^{13}C\{^1H\}$ NMR ($CDCl_3$): δ 28.22 ($C[CH_3]_3$, major isomer), 28.36 ($C[CH_3]_3$, minor isomer), 29.06 ($C[CH_3]_3$, minor isomer), 29.18 ($C[CH_3]_3$, major isomer), 35.13 ($C[CH_3]_3$, minor isomer), 35.46 ($C[CH_3]_3$, major isomer), 35.48 ($C[CH_3]_3$, minor isomer), 35.62 ($C[CH_3]_3$, minor isomer), 113.60, 120.81 (sept, $^3J_{CF}$ = 4 Hz, terphenyl 4,4′′-C, minor isomer), 121.07 (sept, $^3J_{CF}$ = 4 Hz, terphenyl 4,4′′-C, major isomer), 123.42 (q, $^1J_{CF}$ = 273 Hz, CF_3, major isomer), 123.52 (q, $^1J_{CF}$ = 273 Hz, CF_3, minor isomer), 123.69, 124.42, 125.59, 126.18, 128.84, 129.88 (q, $^3J_{CF}$ = 3 Hz, terphenyl 2,6,2′′,6′′-C, minor isomer), 129.99 (q, $^3J_{CF}$ = 3 Hz, terphenyl 2,6,2′′,6′′-C, major isomer), 130.91, 131.50 (q, $^2J_{CF}$ = 33 Hz, terphenyl 3,5,3′′,5′′-C, minor isomer), 131.73 (q, $^2J_{CF}$ = 33 Hz, terphenyl 3,5,3′′,5′′-C, minor isomer), 132.80, 134.66, 141.01, 141.60, 146.29, 147.54, 149.47, 149.54, 155.35, 156.78, 157.29, 158.20, 178.76 (*C*=O, minor isomer), 182.10 (*C*=O, major isomer). $^{19}F\{^1H\}$ NMR ($CDCl_3$): δ –63.38. IR (evapd film, cm^{-1}): 3065 (w), 2964 (m), 2912 (w), 2864 (w), 1665 (w), 1618 (w), 1575 (w), 1546 (w), 1474 (w), 1450 (w), 1369 (s), 1274 (s), 1173 (s), 1135 (s), 1054 (w), 1021 (w), 963 (w), 892 (m), 858 (w), 844 (w), 801 (w), 787 (w), 782 (w), 768 (w), 744 (w), 739 (w), 706 (m), 782 (m), 658 (w). UV-Vis (CH_2Cl_2): λ_{max} = 409 nm (ε = 4600 L mol^{-1} cm^{-1}), 304 (11000). Anal. Calcd for $C_{36}H_{29}F_{12}NO$: C, 60.09; H, 4.06; N, 1.95. Found: C, 59.30; H, 4.11; N, 1.94.

***Cis*- and *trans*-dichlorobis(*N*-2'-(3,5,3'',5''-tetrakis(trifluoromethyl)-*m*-terphenyl)-3,5-di-*tert*-butyl-1,2-benzoiminoxolene)ruthenium, $(CF_3Tio)_2RuCl_2$.** A mixture of 180 mg $\{(cymene)RuCl_2\}_2$ (0.588 mmol Ru) and 921 mg CF_3Tio (1.280 mmol, 2.18 equiv) is dissolved in 15 mL dry toluene in the glovebox. The mixture is placed in a 20 mL scintillation vial with a

stirbar, sealed, and heated with stirring in a 110 °C oil bath for 4 d. The vial is then opened to the air and the volatiles removed on a rotary evaporator. 7 mL of $CHCl_3$ is added to the residue and the mixture allowed to stand for 1 hr. The insoluble material is collected by suction filtration and washed with 3 × 10 mL of $CHCl_3$ to afford pure ***trans*-$(CF_3Tio)_2RuCl_2$** (84 mg, 9%). ^1H NMR (CD_2Cl_2): δ 1.16 (s, 18H, ^{t}Bu), 1.32 (s, 18H, ^{t}Bu), 7.13 (d, 1.8 Hz, 2H, iminoxolene 3- or 5-H), 7.27 (d, 7.7 Hz, 4H, Ar 4',6'-H), 7.38 (d, 1.8 Hz, 2H, iminoxolene 3- or 5-H), 7.49 (d, 1.6 Hz, 8H, Ar 2,6,2",6"-H) 7.51 (t, 7.9 Hz, 2H, Ar 5'-H), 7.60 (t, 1.5 Hz, 4H, Ar 4,4"-H). The pure *trans* isomer is too insoluble for ^{13}C spectroscopy. $^{19}F\{^1H\}$ NMR (CD_2Cl_2): δ –63.27 (s, 24F). IR (ATR, cm^{-1}): 2969 (w), 2912 (w), 2867 (w), 1372 (m), 1355 (w), 1290 (w), 1279 (s), 1175 (m), 1124 (s), 1098 (w), 1074 (w), 1025 (w), 992 (w), 943 (w), 904 (m), 895 (m), 873 (w), 847, (w), 819 (w), 823 (w), 791 (w), 740 (w), 703 (m), 699 (m), 690 (m). UV-Vis-NIR (CH_2Cl_2): λ_{max} = 1106 nm (ε = 7900 L mol^{-1} cm^{-1}), 816 (18000), 499 (sh, 4300), 386 (7900). Anal. Calcd for $C_{74}H_{66}Cl_2F_{24}N_2O_2Ru$: C, 54.09; H, 4.05; N, 1.70. Found: C, 54.26; H, 3.62; N, 1.77.

The blue filtrate is evaporated using a rotary evaporator. The blue residue is slurried with approximately 10 mL of acetonitrile and the solid collected by vacuum filtration through a glass frit. Washing with 2 × 10 mL acetonitrile and air-drying for 30 min gives 460 mg (48%) of a mixture of ***cis*- and *trans*-$(CF_3Tio)_2RuCl_2$** (5:1 ratio of *cis*:*trans* by ^1H NMR). ^1H NMR (*cis* isomer, CD_2Cl_2): δ 1.05 (s, 18H, ^{t}Bu), 1.16 (s, 18H, ^{t}Bu), 7.05 (d, 2.1 Hz, 2H, iminoxolene 3- or 5-H), 7.49 (dd, 7.7, 1.5 Hz, 2H, Ar 4'- or 6'-H), 7.52 (dd, 8.4, 1.5 Hz, 2H, Ar 4'- or 6'-H), 7.56 (sl br, 4H, Ar 4,4"-H), 7.60 (br, 8H, Ar 2,6,2",6"-H), 7.70 (t, 7.7 Hz, 2H, Ar 5'-H). $^{13}C\{^1H\}$ NMR (CD_2Cl_2): δ 28.75, 29.19, 29.26, 29.78, 34.52, 34.49, 34.95. 35.53, 113.37, 113.78, 120.69 (broad), 121.04 (broad), 121.18 (broad), 122.82 (q, $^1J_{CF}$ = 273 Hz), 123.32 (q, $^1J_{CF}$ = 273 Hz), 123.55 (q, $^1J_{CF}$ = 273 Hz), 125.37, 127.41, 128.29, 129.01, 129.09 (q, $^2J_{CF}$ = 34 Hz), 129.94

(broad), 130.19 (q, $^2J_{CF}$ = 33 Hz), 130.25, 130.99, 131.15 (q, $^2J_{CF}$ = 33 Hz), 132.44, 132.50, 133.31, 133.92, 135.10, 135.15, 140.33, 141.07, 141.56, 144.34, 145.30, 146.15, 146.23, 152.02, 153.34, 164.10, 169.57, 182.27, 192.94. $^{19}F\{^1H\}$ NMR (*cis* isomer, CD_2Cl_2): δ –62.93 (s, 12F), –63.02 (br s, 12F). IR (evapd film, cm^{-1}): 2967 (m), 2915 (m), 2877 (w), 1797 (w), 1615 (w), 1590 (m), 1521 (m), 1478 (m), 1461 (m), 1397 (w), 1367 (s), 1306 (w), 1281 (s), 1173 (s), 1122 (s), 1096 (s), 1066 (w), 1023 (m), 989 (w), 890 (m), 869 (w), 843 (w), 800 (w), 736 (m), 702 (m), 676 (m), 637 (w). UV-Vis-NIR (*cis* isomer, CH_2Cl_2): λ_{max} = 656 nm (ε = 28000 L mol^{-1} cm^{-1}).

Bis(*N*-(2,6-diisopropylphenyl)-3,5-di-*tert*-butyl-2-benzoiminoxolene)(triphenylphosphine)ruthenium, (Diso)$_2$Ru(PPh$_3$). *cis*-(Diso)$_2$RuCl$_2$ (100 mg, 0.107 mmol) and cobaltocene (42 mg, 0.222 mmol, 2.07 equiv) are dissolved in 6 mL THF in the glovebox. The solution is shaken to dissolve the materials and immediately turns pink. It is then added to 61 mg solid triphenylphosphine (0.236 mmol, 2.2 equiv) in a 20-mL glass scintillation vial. The vial is capped and stirred for 2 d at room temperature. After filtration of the reaction mixture through a glass frit, the filtrate is collected, transferred to a round bottom flask, and stripped to dryness on the vacuum line. The green residue is dissolved in a vial with 3 mL CH_2Cl_2 and layered with 9 mL of CH_3CN. After 1 d at room temperature, the green crystals are collected on a glass frit by suction filtration, washed with 2 × 2 mL CH_3CN, and air-dried to give 85.2 mg of (Diso)$_2$Ru(PPh$_3$) (71%). ^1H NMR (CD_2Cl_2, –85 °C): δ –0.08 (d, 6.7 Hz, 3H, CH(C*H*$_3$)$_2$), 0.09 (d, 6.4 Hz, 3H, CH(C*H*$_3$)$_2$), 0.17 (d, 6.5 Hz, 3H, CH(C*H*$_3$)$_2$), 0.39 (d, 6.6 Hz, 3H, CH(C*H*$_3$)$_2$), 0.56 (d, 6.9 Hz, 3H, CH(C*H*$_3$)$_2$), 0.70 (d, 6.6 Hz, 3H, CH(C*H*$_3$)$_2$), 0.83 (d, 6.7 Hz, 3H, CH(C*H*$_3$)$_2$), 0.89 (s, 9H, ^{t}Bu), 1.00 (s, 9H, ^{t}Bu), 1.02 (s, 9H, ^{t}Bu), 1.15 (s, 9H, ^{t}Bu), 1.46 (sept, 6.6 Hz, 1H, C*H*(CH$_3$)$_2$), 1.94 (sept, 6.2 Hz, 1H, C*H*(CH$_3$)$_2$), 2.35 (sept, 6.4 Hz, 1H,

C*H*(CH_3)$_2$), 5.98 (broad, 2H, PPh_3), 6.21 (d, 1.8 Hz, 1H, iminoxolene 3- or 5-H), 6.45 (d, 1.4 Hz, 1H, iminoxolene 3- or 5-H), 6.63 (t, 8.7 Hz, 1H, *p*-H PPh_3), 6.81 (broad, 2H, PPh_3), 6.91-7.40 (m, 14H), 7.51 (t, 7.6 Hz, 2H), 7.62 (m, 1H, PPh_3), 8.47 (dd, 13.5 Hz, 7.5 Hz, 1H, PCC*H*). One CH(C*H*$_3$) and one C*H*(CH_3)$_2$ signal are not observed, presumably because they are obscured by ^{t}Bu peaks. $^{31}P\{^1H\}$ NMR (CD_2Cl_2): δ 48.34. IR (nujol mull, cm^{-1}): 3165 (w), 1587 (m), 1541 (m), 1317 (m), 1294 (m), 1253 (m), 1229 (m), 1199 (s), 1158 (s), 1103 (w), 1092 (s), 1026 (w), 996 (w), 867 (m), 799 (m), 777 (m), 742 (m), 722 (w), 692 (m). UV-Vis-NIR (CH_2Cl_2): λ_{max} = 713 nm (ε = 13100 L mol^{-1} cm^{-1}), 436 (7300), 543 (4000). Anal. Calcd for $C_{70}H_{89}N_2O_2PRu$: C, 74.90; H, 7.99; N, 2.50. Found: C, 74.04; H, 8.27; N, 2.61.

Bis(*N*-(2,6-diisopropylphenyl)-3,5-di-*tert*-butyl-1,2-benzoiminoxolene)(triphenylphosphine)osmium, (Diso)$_2$Os(PPh$_3$). The osmium compound is prepared by the method used for the ruthenium analogue using 100 mg of *cis*-(Diso)$_2$$OsCl_2$ (0.107 mmol), 40 mg of Cp_2Co (0.211 mmol, 2.15 equiv), and 58 mg of PPh_3 (0.221 mmol, 2.25 equiv), and yields 79.2 mg of (Diso)$_2$Os(PPh_3) (67%). ^{1}H NMR (CD_2Cl_2, –78 °C): δ –0.29 (d, 5.7 Hz, 3H, CH(C*H*$_3$)$_2$), –0.03 (d, 6.2 Hz, 3H, CH(C*H*$_3$)$_2$), 0.17 (d, 6.4 Hz, 3H, CH(C*H*$_3$)$_2$), 0.39 (d, 6.5 Hz, 3H, CH(C*H*$_3$)$_2$), 0.50 (d, 6.0 Hz, 3H, CH(C*H*$_3$)$_2$), 0.73 (d, 6.4 Hz, 3H, CH(C*H*$_3$)$_2$), 0.76 (d, 6.2 Hz, 3H, CH(C*H*$_3$)$_2$), 0.94 (d, 6.5 Hz, 3H, CH(C*H*$_3$)$_2$), 0.98 (s, 9H, ^{t}Bu), 1.05 (s, 18H, 2 × ^{t}Bu), 1.20 (s, 9H, ^{t}Bu), 1.34 (sept, 6.4 Hz, 1H, C*H*(CH_3)$_2$), 1.46 (sept, 6.4 Hz, 1H, C*H*(CH_3)$_2$), 2.13 (sept, 6.6 Hz, 1H, C*H*(CH_3)$_2$), 5.76 (br, 2H, PPh_3), 6.06 (d, 1.5 Hz, 1H, iminoxolene 3- or 5-H), 6.16 (d, 1.4 Hz, 1H, iminoxolene 3- or 5-H), 6.19 (br, 1H, PPh_3), 6.48 (d, 1.9 Hz, 1H, iminoxolene 3- or 5-H), 6.57 (br, 1H, PPh_3), 6.60 (t, 7.8 Hz, 1H, PPh_3), 6.82 (d, 7.4 Hz, 1H, Ar 3- or 5-H), 6.90 (d, 2.0 Hz, 1H, iminoxolene 3- or 5-H), 7.07-7.46 (m, 13H), 7.84 (br, 1H, PPh_3), 7.93 (dd, 12.3 Hz, 7.8 Hz, 1H, PCC*H*). One C*H*(CH_3)$_2$ signal is not observed,

presumably because it is obscured by a ^{t}Bu peak. $^{31}P\{^1H\}$ NMR (CD_2Cl_2): δ –18.59. IR (nujol mull, cm^{-1}): 3058 (w), 1587 (w), 1551 (w), 1316 (m), 1278 (w), 1254 (m), 1232 (w), 1199 (m), 1158 (m), 1092 (w), 866 (w), 800 (m), 770 (w), 744 (m), 692 (m). UV-Vis-NIR (CH_2Cl_2): λ_{max} = 796 nm (ε = 1400 L mol^{-1} cm^{-1}), 608 nm (20200), 483 (6900), 414 (8600), 371 (sh, 9800). Anal. Calcd for $C_{70}H_{89}N_2O_2OsP$: C, 69.39; H, 7.40; N, 2.31. Found: C, 69.08; H, 7.37; N, 2.24.

Electrochemistry. Electrochemical measurements were performed in the drybox using a Metrohm Autolab PGSTAT128N potentiostat. A standard three-electrode setup was used, with glassy carbon working and counter electrodes and a silver/silver chloride pseudo-reference electrode. The electrodes were connected to the potentiostat through electrical conduits in the drybox wall. Samples were 1 mM in CH_2Cl_2 with 100 mM $[Bu_4N]PF_6$ as supporting electrolyte. Potentials were referenced to ferrocene/ferrocenium at 0 V,[S5] with the reference potential established by spiking the solutions of *cis*- and *trans*-$(Diso)_2RuCl_2$ with a small amount of ferrocene ($E°$ = 0 V) and the solutions of *trans*-$(CF_3Tio)_2RuCl_2$, $(Diso)_2Ru(PPh_3)$, and $(Diso)_2Os(PPh_3)$ with a small amount of decamethylferrocene ($E°$ = –0.565 V).[S6] Cyclic voltammograms were recorded with a scan rate of 60 mV s^{-1}.

Variable-temperature NMR spectroscopy. Variable-temperature ^1H NMR spectra of $(Diso)_2M(PPh_3)$ (M = Ru, Os) were measured on CD_2Cl_2 solutions on a Bruker Avance DPX-400 NMR spectrometer, with temperatures calibrated using the peak separation in CH_3OH.[S7] Variable-temperature ^1H NMR spectra of *trans*-$(Diso)_2MCl_2$ (M = Ru, Os) were measured on solutions in 20% $CDFCl_2$/80% CF_2Cl_2 in flame-sealed glass NMR tubes. Temperatures were calibrated down to 178 K using the peak separation in CH_3OH as described above. To calibrate temperatures below 178 K, the peak separation between the ^{13}C signals in $(Me_3Si)_3CH$ in the

20% $CDFCl_2$/80% CF_2Cl_2 solvent system was measured in the range 295-178 K and was found to show a linear dependence on temperature, as had been previously observed in a variety of solvents down to 134 K.[S8] The linear calibration curve was then extrapolated below 178 K and the measured $\Delta\delta$ values used to relate the nominal spectrometer temperature to the actual temperature.

Lineshapes of *trans*-$(Diso)_2RuCl_2$, $(Diso)_2Ru(PPh_3)$, and $(Diso)_2Os(PPh_3)$ were simulated using iNMR. For *trans*-$(Diso)_2OsCl_2$, the iminoxolene proton resonances at 129 and 137 K were simulated in iNMR, and the isopropyl methine resonances at 120, 146, and 164 K were simulated using the dynamic NMR simulation routine in Topspin. In the spectra of $(Diso)_2Ru(PPh_3)$ and $(Diso)_2Os(PPh_3)$, the *tert*-butyl protons were simulated. For *trans*-$(Diso)_2RuCl_2$, the chemical shifts of the exchanging downfield iminoxolene protons were determined by lineshape simulation at 100 K, and that difference in chemical shift was assumed to be independent of temperature in simulations of spectra at higher temperatures. For all other spectra, at temperatures above the coalescence point, chemical shifts of exchanging signals were estimated by linear extrapolation of the shifts observed below the coalescence point, and the extrapolated difference in chemical shift was treated as fixed in the simulation.

Calculations. Geometry optimizations and orbital calculations used the hybrid B3LYP method, using the Gaussian16 suite of programs.[S9] An SDD basis set was used for ruthenium and osmium and a 6-31G* basis set for all other atoms. Ligands were truncated by using 1,2-$C_6H_4(NH)O$ (ap) as the iminoxolene, and PMe_3 was used in place of PPh_3. Optimized geometries were confirmed to be minima by frequency analysis. For *trans*-$(ap)_2MCl_2$, the minimum-energy structures had C_s symmetry. Structures constrained to adopt C_2 symmetry were at higher energy, and were found to be transition states (one imaginary frequency) leading to the interconversion of the two equivalent C_s structures. Constraining *trans*-$(ap)_2MCl_2$ to C_i or

C_{2h} symmetry led to essentially identical optimized structures, at higher energy than the C_2-symmetric structures. Calculations on $(ap)_2Os(PMe_3)$ have been previously reported.[S10] Constrained calculations on $(ap)_2M(PMe_3)$ required the $(ap)_2MP$ core to adhere to C_2 symmetry, but the methyl groups on phosphorus were allowed to refine freely. Plots of calculated Kohn-Sham orbitals were generated using the program GaussView (v. 6.0.16) with an isovalue of 0.04.

II. X-ray crystallography

Crystallographic details. Crystals of *cis*-$(Diso)_2RuCl_2$ and *cis*-$(Diso)_2OsCl_2$ were grown by vapor diffusion of acetonitrile into benzene solutions of the compounds, while crystals of *trans*-$(Diso)_2RuCl_2$ deposited from the crude reaction mixture dissolved in hexane. Crystals of *trans*-$(^{CF3}Tio)_2RuCl_2$, $(Diso)_2Os(PPh_3)$•2 CH_2Cl_2, and $(Diso)_2Ru(PPh_3)$•2 CH_2Cl_2 were grown by liquid diffusion of acetonitrile into dichloromethane solutions of the complexes. Crystals of CF_3Tio deposited from a methanol solution of the compound at room temperature. Crystals were placed in Paratone oil before being transferred to the cold N_2 stream of a Bruker Apex II CCD diffractometer in a nylon loop. Data were reduced, correcting for absorption, using the program SADABS. The structures were solved using Patterson methods, with remaining nonhydrogen atoms found on difference Fourier maps, and all nonhydrogen atoms were refined anisotropically. Hydrogen atoms were found on difference Fourier maps and refined isotropically, except for those in *trans*-$(Diso)_2RuCl_2$ and those on the lattice solvent and disordered *tert*-butyl group in $(Diso)_2Ru(PPh_3)$•2 CH_2Cl_2, which were placed in calculated positions.

In *trans*-$(Diso)_2RuCl_2$, iminoxolene ring 2 is disordered in two different orientations. Atoms C23, C24, C25, and the *tert*-butyl group centered at C28 are in different positions in the two components. Corresponding atoms in the two components were given identical thermal parameters, and the occupancy of the two components was allowed to vary, refining to 55.4(4)% occupancy of the major component. In $(Diso)_2Ru(PPh_3)$•2 CH_2Cl_2, one lattice CH_2Cl_2 was refined at full occupancy, while another near the inversion center was refined in three positions constrained to sum to a single CH_2Cl_2. One *tert*-butyl group (the one centered on C18) in this structure was modeled as occupying two orientations. In $(Diso)_2Os(PPh_3)$•2 CH_2Cl_2, one lattice

CH_2Cl_2 and was refined at full occupancy, while solvent in a channel near the inversion center was too disordered to model, The diffuse electron density in this channel was treated with the program SQUEEZE.[S11] The volume of solvent in the asymmetric unit was 212 $Å^3$ and the electron count was 46, corresponding to one molecule of CH_2Cl_2 per asymmetric unit. One *tert*-butyl group (the one centered on C18) in this structure was modeled as occupying two orientations. In CF_3Tio, the oxygen atom (O and O1) was modeled in two different positions on the iminoquinone ring, corresponding to the (*Z*) and (*E*) isomers, in a 10:1 ratio. One of the CF_3 groups (bonded to C471) also showed slight disorder, with the minor component refined with fixed C–F distances and with thermal parameters pinned to those in the major component; the refined population of the minor component was 8.0(3)%. In *trans*-$(CF_3Tio)_2RuCl_2$, four of the trifluoromethyl groups (the ones centered on C318, C417, C418, C427) in the structure showed rotational disorder and were modeled as occupying two orientations. Calculations used SHELXTL (Bruker AXS),[S12] with scattering factors and anomalous dispersion terms taken from the literature.[S13] Further details may be found in Tables S1-S4, with summaries of bond distances and angles in Tables S5-S7.

Table S1. Crystal data for *cis*-$(Diso)_2RuCl_2$ and *cis*-$(Diso)_2OsCl_2$.

	cis-$(Diso)_2RuCl_2$	*cis*-$(Diso)_2OsCl_2$
Molecular formula	$C_{52}H_{74}Cl_2N_2O_2Ru$	$C_{52}H_{74}Cl_2N_2O_2Os$
Formula weight	931.10	1020.23
T/K	120(2)	120(2)
Crystal system	Monoclinic	Monoclinic
Space group	$P2_1/c$	$P2_1/c$
λ/Å	0.71073 (Mo Kα)	0.71073 (Mo Kα)
Total data collected	67806	514155
No. of indep. reflns.	12376	46238
R_{int}	0.0521	0.0409
Obsd refls [$I > 2\sigma(I)$]	10496	39851
a/Å	18.8219(8)	18.7953(9)
b/Å	12.0482(5)	12.0376(5)
c/Å	22.0868(10)	22.1480(10)
α/°	90	90
β/°	92.6706(17)	92.0871(17)
γ/°	90	90
V/Å^3	5003.2(4)	5007.7(4)
Z	4	4
μ/mm^{-1}	0.459	2.692
Crystal size/mm	0.23 × 0.19 × 0.17	0.29 × 0.28 × 0.27
No. refined parameters	828	828
$R1$, $wR2$ [$I > 2\sigma(I)$]	0.0317, 0.0634	0.0256, 0.0483
$R1$, $wR2$ [all data]	0.0426, 0.0686	0.0354, 0.0507
Goodness of fit	1.092	1.198

Table S2. Crystal data for *trans*-$(Diso)_2RuCl_2$ and *trans*-$(Diso)_2OsCl_2$.

	trans-$(Diso)_2RuCl_2$	*trans*-$(Diso)_2OsCl_2$
Molecular formula	$C_{52}H_{74}Cl_2N_2O_2Ru$	$C_{52}H_{74}Cl_2N_2O_2Os$
Formula weight	931.10	1020.23
T/K	120(2)	120(2)
Crystal system	Monoclinic	Monoclinic
Space group	$P2_1/c$	$P2_1/c$
λ/Å	0.71073 (Mo Kα)	0.71073 (Mo Kα)
Total data collected	74920	110676
No. of indep. reflns.	12967	11561
R_{int}	0.0606	0.0441
Obsd refls [$I > 2\sigma(I)$]	10562	10532
a/Å	17.1927(11)	17.3519(19)
b/Å	22.2351(14)	22.294(3)
c/Å	13.9010(9)	13.7682(15)
α/°	90	90
β/°	100.305(2)	100.3577(17)
γ/°	90	90
V/Å^3	5228.4(6)	5239.4(10)
Z	4	4
μ/mm^{-1}	0.439	2.573
Crystal size/mm	0.19 × 0.12 × 0.10	0.21 × 0.15 × 0.10
No. refined parameters	554	596
$R1$, $wR2$ [$I > 2\sigma(I)$]	0.0717, 0.1315	0.0625, 0.1270
$R1$, $wR2$ [all data]	0.0900, 0.1389	0.0694, 0.1297
Goodness of fit	1.210	1.302

Table S3. Crystal data for CF_3Tio and *trans*-$(CF_3Tio)_2RuCl_2$.

	CF_3Tio	*trans*-$(CF_3Tio)_2RuCl_2$
Molecular formula	$C_{36}H_{29}F_{12}NO$	$C_{72}H_{58}Cl_2F_{24}N_2O_2Ru$
Formula weight	719.60	1611.17
T/K	120(2)	200(2)
Crystal system	Orthorhombic	Triclinic
Space group	*Pbca*	$P\bar{1}$
λ/Å	0.71073 (Mo Kα)	0.71073 (Mo Kα)
Total data collected	146007	58028
No. of indep. reflns.	8290	19265
R_{int}	0.0360	0.0302
Obsd refls [$I > 2\sigma(I)$]	7145	15573
a/Å	20.2437(13)	13.2962(13)
b/Å	9.7698(6)	13.5768(14)
c/Å	33.781(3)	21.676(2)
α/º	90	76.1839(15)
β/º	90	82.2455(15)
γ/º	90	68.8954(14)
V/Å^3	6681.0(8)	3539.7(6)
Z	8	2
μ/mm^{-1}	0.132	0.407
Crystal size/mm	0.39 × 0.33 × 0.16	0.19 × 0.16 × 0.09
No. refined parameters	581	1200
$R1$, $wR2$ [$I > 2\sigma(I)$]	0.0471, 0.1098	0.0391, 0.0870
$R1$, $wR2$ [all data]	0.0561, 0.1156	0.0556, 0.0943
Goodness of fit	1.070	1.019

Table S4. Crystal data for $(Diso)_2Ru(PPh_3) \cdot 2\ CH_2Cl_2$ and $(Diso)_2Os(PPh_3) \cdot 2\ CH_2Cl_2$

	$(Diso)_2Ru(PPh_3) \cdot 2\ CH_2Cl_2$	$(Diso)_2Os(PPh_3) \cdot 2\ CH_2Cl_2$
Molecular formula	$C_{72}H_{93}Cl_4N_2O_2PRu$	$C_{72}H_{93}Cl_4N_2O_2OsP$
Formula weight	1292.32	1381.45
T/K	120(2)	120(2)
Crystal system	Triclinic	Triclinic
Space group	$P\bar{1}$	$P\bar{1}$
λ/Å	0.71073 (Mo Kα)	0.71073 (Mo Kα)
Total data collected	106405	53324
No. of indep. reflns.	16961	17058
R_{int}	0.0311	0.0227
Obsd refls [$I > 2\sigma(I)$]	15197	15759
a/Å	11.6411(12)	11.6271(13)
b/Å	15.7348(16)	15.7458(18)
c/Å	20.953(2)	20.984(2)
α/°	101.7895(16)	101.7330(16)
β/°	101.1562(17)	101.0916(16)
γ/°	107.3093(16)	107.4927(16)
V/Å^3	3451.5(6)	3452.8(7)
Z	2	2
μ/mm^{-1}	0.449	2.069
Crystal size/mm	0.27 × 0.21 × 0.12	0.36 × 0.24 × 0.11
No. refined parameters	1090	1042
$R1$, $wR2$ [$I > 2\sigma(I)$]	0.0348, 0.0931	0.0239, 0.0613
$R1$, $wR2$ [all data]	0.0407, 0.0968	0.0273, 0.0626
Goodness of fit	1.062	1.059

Table S5. Selected bond distances (Å), angles (°), and metrical oxidation states (MOS)[S14] for *cis*-(Diso)$_2$RuCl$_2$ and *cis*-(Diso)$_2$OsCl$_2$. Values given in Roman type are from the crystal structures. Values given in italics are from DFT calculations on *cis*-(ap)$_2$MCl$_2$ (ap = $C_6H_4(NH)O$), which are C_2-symmetric.

Parameter	*cis*-(Diso)$_2$**Ru**Cl$_2$		*cis*-(Diso)$_2$**Os**Cl$_2$	
	X-ray	*DFT*	X-ray	*DFT*
M–O1	2.0272(12)	*2.0742*	2.0047(6)	*2.0550*
M–O2	2.0290(12)		2.0109(6)	
M–N1	2.0179(14)	*1.9791*	2.0120(7)	*1.9803*
M–N2	2.0156(14)		2.0068(6)	
M–Cl1	2.3236(4)	*2.3514*	2.3168(2)	*2.3612*
M–Cl2	2.3234(4)		2.3184(2)	
C11–O1	1.287(2)	*1.2814*	1.3048(10)	*1.3004*
C12–N1	1.342(2)	*1.3271*	1.3558(10)	*1.3448*
C11–C12	1.445(2)	*1.4587*	1.4298(11)	*1.4407*
C12–C13	1.421(2)	*1.4286*	1.4142(11)	*1.4192*
C13–C14	1.365(3)	*1.3691*	1.3725(12)	*1.3761*
C14–C15	1.441(3)	*1.4346*	1.4285(13)	*1.4252*
C15–C16	1.370(2)	*1.3727*	1.3818(12)	*1.3793*
C11–C16	1.437(2)	*1.4252*	1.4220(11)	*1.4151*
C21–O2	1.283(2)	*1.2814*	1.3057(10)	*1.3004*
C22–N2	1.339(2)	*1.3271*	1.3554(10)	*1.3448*
C21–C22	1.446(2)	*1.4587*	1.4283(11)	*1.4407*
C22–C23	1.424(2)	*1.4286*	1.4125(11)	*1.4192*
C23–C24	1.363(2)	*1.3691*	1.3712(12)	*1.3761*
C24–C25	1.437(3)	*1.4346*	1.4250(13)	*1.4252*
C25–C26	1.370(3)	*1.3727*	1.3842(12)	*1.3793*
C21–C26	1.440(2)	*1.4252*	1.4222(11)	*1.4151*
Cl1–M–Cl2	91.449(17)	*91.27*	91.073(9)	*89.39*
O1–M–N1	78.04(5)	*77.20*	77.84(3)	*76.73*
O2–M–N2	78.15(5)		78.18(3)	
O1–M–N2	93.51(5)	*96.77*	93.04(3)	*93.03*
O2–M–N1	93.58(5)		93.39(3)	
N1–M–N2	168.76(6)	*171.03*	168.09(3)	*164.03*
O1–M–O2	84.99(5)	*97.09*	85.96(3)	*101.01*
MOS, Ring 1	–0.80(4)	*–0.70(6)*	–1.10(4)	*–1.01(5)*
MOS, Ring 2	–0.76(5)		–1.12(4)	

Table S6. Selected bond distances (Å), angles (°), and metrical oxidation states (MOS)[S14] for *trans*-(iminoxolene)$_2$RuCl$_2$. Values given in Roman type are from the crystal structures. Values given in italics are from DFT calculations on *trans*-(ap)$_2$RuCl$_2$ (ap = C$_6$H$_4$(NH)O). Values in *red* are from calculations on compounds constrained to have C_2 symmetry and those in *blue* are constrained to have C_{2h} (or C_i) symmetry.

Parameter	*trans*-(Diso)$_2$RuCl$_2$ X-ray	*trans*-(CF$_3$Tio)$_2$RuCl$_2$, X-ray	trans-*(ap)$_2$RuCl$_2$ DFT (minimum-energy, C$_s$)*	trans-*(ap)$_2$RuCl$_2$ DFT (C_2)*	trans-*(ap)$_2$RuCl$_2$ DFT (C_{2h})*
Ru–O1	2.079(2)	2.0545(13)	*2.1171*	*2.0660*	*2.0851*
Ru–O2	1.966(3)	1.9548(12)	*1.9903*		
Ru–N1	1.949(3)	1.9671(14)	*1.9327*	*2.0016*	*2.0063*
Ru–N2	2.064(4)	2.1069(14)	*2.0994*		
Ru–Cl1	2.3346(10)	2.3082(5)	*2.3610*	*2.4089*	*2.4109*
Ru–Cl2	2.3347(10)	2.3207(5)		*2.4104*	
C11–O1	1.279(4)	1.273(2)	*1.2780*	*1.2703*	*1.2649*
C12–N1	1.339(4)	1.339(2)	*1.3342*	*1.3167*	*1.3137*
C11–C12	1.449(5)	1.457(2)	*1.4594*	*1.4761*	*1.4802*
C12–C13	1.408(5)	1.418(2)	*1.4259*	*1.4345*	*1.4362*
C13–C14	1.351(5)	1.361(3)	*1.3700*	*1.3644*	*1.3632*
C14–C15	1.442(5)	1.440(3)	*1.4331*	*1.4419*	*1.4442*
C15–C16	1.368(5)	1.364(3)	*1.3730*	*1.3673*	*1.3659*
C11–C16	1.439(4)	1.442(2)	*1.4275*	*1.4318*	*1.4346*
C21–O2	1.286(5)	1.292(2)	*1.2829*	*1.2703*	*1.2649*
C22–N2	1.325(5)	1.321(2)	*1.3111*	*1.3167*	*1.3137*
C21–C22	*a*	1.457(2)	*1.4690*	*1.4761*	*1.4802*
C22–C23	*a*	1.432(2)	*1.4375*	*1.4345*	*1.4362*
C23–C24	*a*	1.361(3)	*1.3654*	*1.3644*	*1.3632*
C24–C25	*a*	1.446(3)	*1.4393*	*1.4419*	*1.4442*
C25–C26	*a*	1.359(3)	*1.3693*	*1.3673*	*1.3659*
C21–C26	*a*	1.436(2)	*1.4256*	*1.4318*	*1.4346*
Cl1–Ru–Cl2	165.43(4)	168.707(19)	*161.26*	*180*	*180*
O1–Ru–N1	78.57(11)	79.15(5)	*78.35*		
O2–Ru–N2	78.16(14)	78.54(5)	*77.73*		
O1–Ru–N2	109.01(12)	104.55(5)	*107.87*		
O2–Ru–N1	94.76(13)	97.93(6)	*96.05*		
MOS, Ring 1	–0.72(7)	–0.66(5)	*–0.72(5)*	*–0.49(6)*	*–0.42(6)*
MOS, Ring 2	*a*	–0.64(8)	*–0.57(9)*		

[a]Ring 2 is disordered in the X-ray structure of *trans*-(Diso)$_2$RuCl$_2$, so the C–C distances are not measured reliably.

Table S7. Selected bond distances (Å), angles (°), and metrical oxidation states (MOS)[S14] for *trans*-(iminoxolene)$_2$OsCl$_2$. Values given in Roman type are from the crystal structures. Values given in italics are from DFT calculations on *trans*-(ap)$_2$OsCl$_2$ (ap = C_6H_4(NH)O). Values in *red* are from calculations on compounds constrained to have C_2 symmetry and those in *blue* are constrained to have C_{2h} (or C_i) symmetry.

Parameter	*trans*-(Diso)$_2$OsCl$_2$ X-ray	trans-*(ap)$_2$OsCl$_2$ DFT (minimum-energy, C$_s$)*	trans-*(ap)$_2$OsCl$_2$ DFT (C_2)*	trans-*(ap)$_2$OsCl$_2$ DFT (C_{2h})*
Os–O1	2.040(4)	*2.1185*	*2.0513*	*1.9922*
Os–O2	1.955(4)	*1.9872*		
Os–N1	1.949(5)	*1.9435*	*2.0067*	*1.9880*
Os–N2	2.103(6)	*2.1003*		
Os–Cl1	2.3027(16)	*2.3559*	*2.4209*	*2.3666*
Os–Cl2	2.3315(18)		*2.4149*	
C11–O1	1.298(7)	*1.2937*	*1.2870*	*1.3330*
C12–N1	1.355(8)	*1.3497*	*1.3303*	*1.3667*
C11–C12	1.428(9)	*1.4460*	*1.4632*	*1.4303*
C12–C13	1.400(9)	*1.4183*	*1.4273*	*1.4030*
C13–C14	1.362(10)	*1.3757*	*1.3693*	*1.3954*
C14–C15	1.431(10)	*1.4250*	*1.4345*	*1.4042*
C15–C16	1.372(9)	*1.3794*	*1.3723*	*1.3968*
C11–C16	1.430(8)	*1.4186*	*1.4228*	*1.3976*
C21–O2	*a*	*1.3010*	*1.2870*	*1.3330*
C22–N2	*a*	*1.3241*	*1.3303*	*1.3667*
C21–C22	*a*	*1.4535*	*1.4632*	*1.4303*
C22–C23	*a*	*1.4295*	*1.4273*	*1.4030*
C23–C24	*a*	*1.3716*	*1.3693*	*1.3954*
C24–C25	*a*	*1.4313*	*1.4345*	*1.4042*
C25–C26	*a*	*1.3747*	*1.3723*	*1.3968*
C21–C26	*a*	*1.4168*	*1.4228*	*1.3976*
Cl1–Os–Cl2	166.96(8)	*159.43*	*180*	*180*
O1–Os–N1	78.32(19)	*77.66*	*77.21*	*79.51*
O2–Os–N2	78.8(2)	*77.00*		
O1–Os–N2	106.0(2)	*109.22*	*102.63*	*100.49*
O2–Os–N1	96.8(2)	*96.12*		
MOS, Ring 1	–1.03(8)	*–0.97(5)*	*–0.73(6)*	*–1.51(9)*
MOS, Ring 2	*a*	*–0.83(9)*		

[a]Ring 2 is disordered in the X-ray structure of *trans*-(Diso)$_2$OsCl$_2$, so the bond distances are not measured reliably.

Table S8. Selected bond distances (Å), angles (°), and metrical oxidation states (MOS)[S14] for $(Diso)_2Ru(PPh_3)$ and $(Diso)_2Os(PPh_3)$. Values given in Roman type are from the crystal structures. Values given in italics are from DFT calculations on $(ap)_2M(PMe_3)$ (ap = $C_6H_4(NH)O$). Values in red are from calculations where the $(ap)_2M(P)$ substructure is constrained to have C_2 symmetry (the methyl groups cannot adhere to this symmetry and are unconstrained).

Parameter	$(Diso)_2$**Ru**(PPh_3)			$(Diso)_2$**Os**(PPh_3)		
	X-ray	*DFT*	*DFT pseudo-C_2*	X-ray	*DFT*	*DFT pseudo-C_2*
M–O1	2.0852(13)	*2.0832*	*2.0745*	2.0960(15)	*2.1173*	*2.0963*
M–O2	2.0201(12)	*2.0659*		2.0167(15)	*2.0687*	
M–N1	1.9396(15)	*1.9578*	*1.9623*	1.9331(17)	*1.9577*	*1.9661*
M–N2	1.9918(15)	*1.9674*		1.9874(17)	*1.9788*	
M–P	2.2853(5)	*2.2571*	*2.2592*	2.2881(6)	*2.2773*	*2.2771*
C11–O1	1.319(2)	*1.3138*	*1.3124*	1.327(3)	*1.3207*	*1.3183*
C12–N1	1.386(2)	*1.3691*	*1.3680*	1.399(3)	*1.3820*	*1.3788*
C11–C12	1.415(2)	*1.4351*	*1.4358*	1.410(3)	*1.4273*	*1.4290*
C12–C13	1.401(3)	*1.4113*	*1.4119*	1.399(3)	*1.4057*	*1.4074*
C13–C14	1.380(3)	*1.3856*	*1.3851*	1.380(3)	*1.3891*	*1.3876*
C14–C15	1.411(3)	*1.4129*	*1.4136*	1.401(3)	*1.4091*	*1.4110*
C15–C16	1.386(3)	*1.3875*	*1.3870*	1.392(3)	*1.3902*	*1.3888*
C11–C16	1.429(2)	*1.4122*	*1.4125*	1.423(3)	*1.4092*	*1.4099*
C21–O2	1.315(2)	*1.3121*	*1.3124*	1.331(2)	*1.3203*	*1.3183*
C22–N2	1.384(2)	*1.3671*	*1.3680*	1.392(3)	*1.3754*	*1.3788*
C21–C22	1.414(2)	*1.4360*	*1.4358*	1.403(3)	*1.4284*	*1.4290*
C22–C23	1.411(2)	*1.4124*	*1.4119*	1.407(3)	*1.4091*	*1.4074*
C23–C24	1.377(2)	*1.3848*	*1.3851*	1.380(3)	*1.3866*	*1.3876*
C24–C25	1.417(3)	*1.4141*	*1.4136*	1.414(3)	*1.4120*	*1.4110*
C25–C26	1.385(2)	*1.3866*	*1.3870*	1.389(3)	*1.3882*	*1.3888*
C21–C26	1.428(2)	*1.4125*	*1.4125*	1.421(3)	*1.4089*	*1.4099*
O1–M–N1	78.21(6)	*78.69*	*78.74*	77.82(7)	*77.59*	*77.82*
O2–M–N2	79.05(5)	*78.76*		78.81(7)	*77.96*	
O1–M–N2	104.48(5)	*100.69*	*99.81*	103.87(6)	*102.08*	*100.41*
O2–M–N1	92.74(6)	*99.09*		93.01(7)	*98.47*	
N1–M–N2	149.54(6)	*159.73*	*159.29*	148.17(7)	*156.07*	*154.22*
O1–M–O2	167.64(5)	*172.22*	*172.08*	166.69(6)	*170.52*	*172.19*
P–M–O1	83.23(4)	*89.40*	*93.96*	82.34(4)	*84.35*	*93.91*
P–M–O2	108.04(4)	*98.37*		110.23(5)	*105.12*	
P–M–N1	110.41(5)	*103.47*	*100.35*	111.47(5)	*108.19*	*102.89*
P–M–N2	100.00(4)	*96.77*		100.16(5)	*95.49*	
MOS, Ring 1	–1.42(9)	*–1.28(5)*	*–1.27(5)*	–1.59(11)	*–1.39(5)*	*–1.40(6)*
MOS, Ring 2	–1.35(10)	*–1.26(5)*		–1.55(11)	*–1.45(6)*	

Figure S1. Thermal ellipsoid plot of *cis*-$(Diso)_2OsCl_2$, with hydrogen atoms omitted for clarity.

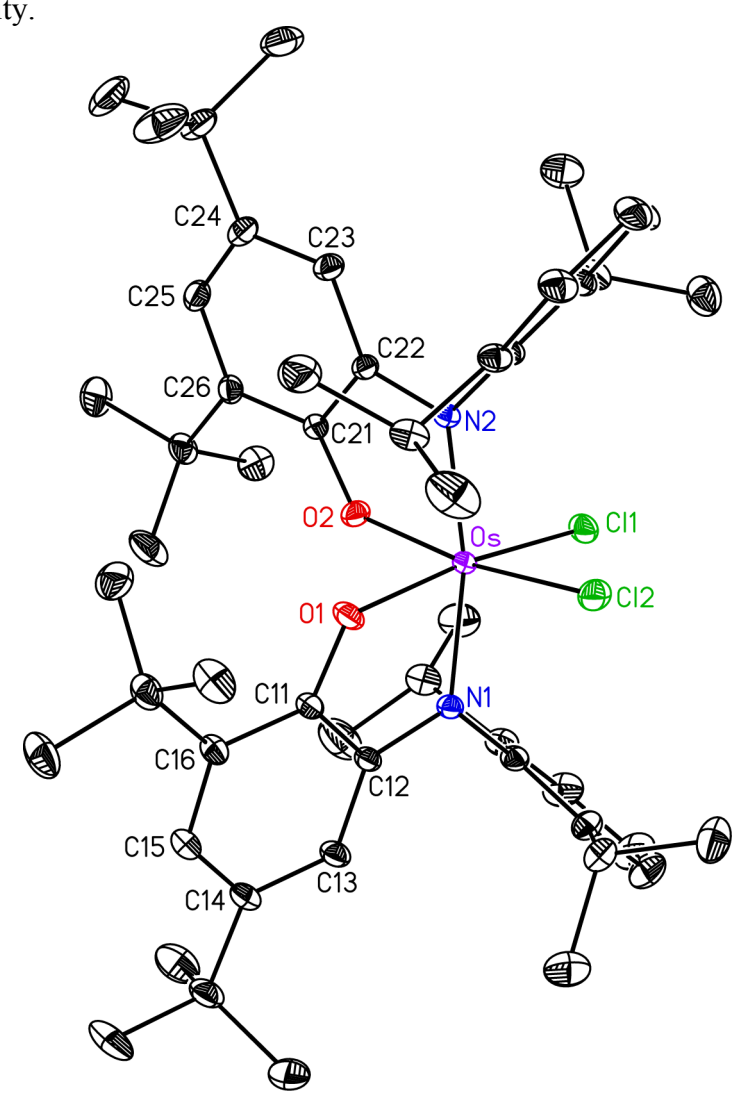

Figure S2. Thermal ellipsoid plot of *trans*-$(Diso)_2OsCl_2$, with hydrogen atoms omitted for clarity. Only one orientation of disordered iminoxolene ring 2 is shown.

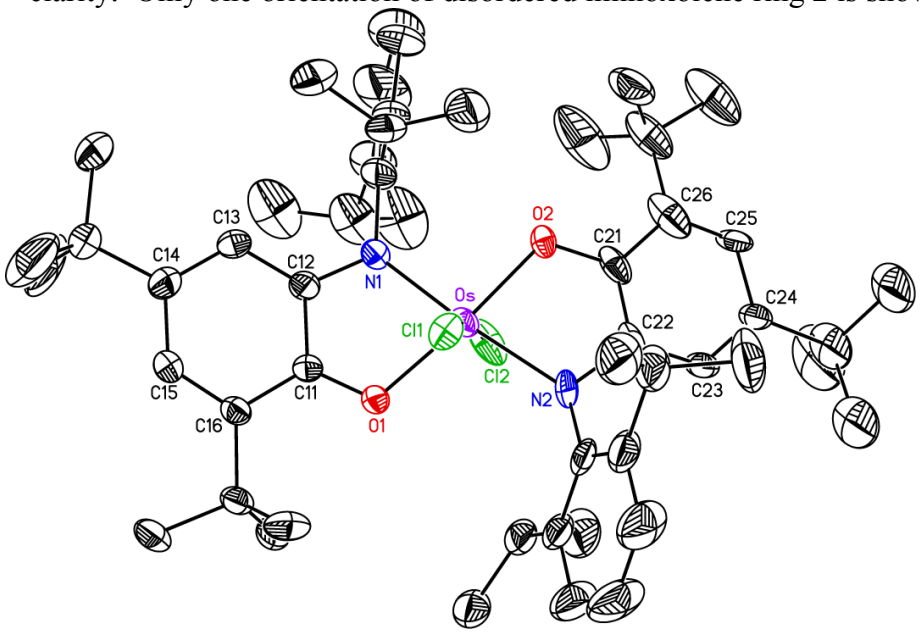

Figure S3. Thermal ellipsoid plot of CF_3Tio, with hydrogen atoms omitted for clarity. Only the major orientation of the iminoquinone and of the disordered CF_3 group centered at C47 is shown.

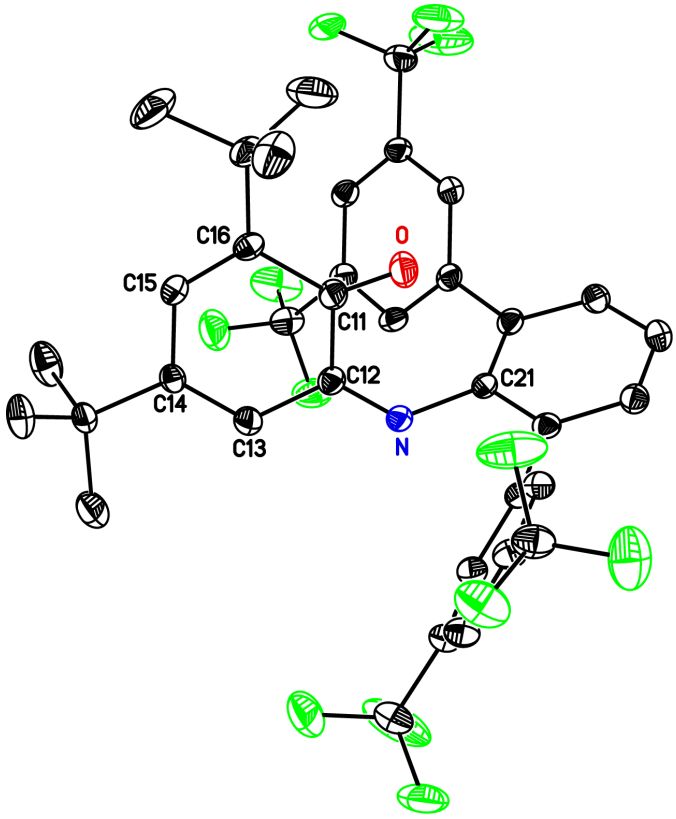

Figure S4. Thermal ellipsoid plot of *trans*-$(CF_3Tio)_2RuCl_2$, with hydrogen atoms omitted for clarity. Only the major orientations of the four disordered CF_3 groups are shown.

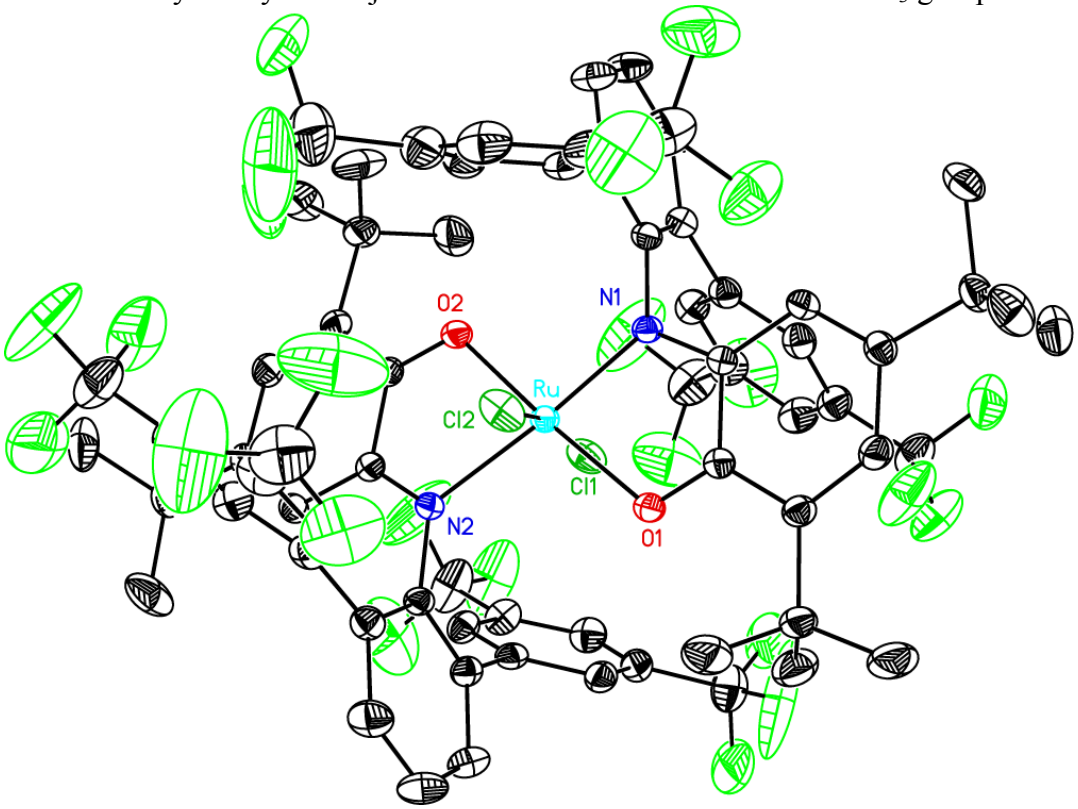

Figure S5. Thermal ellipsoid plot of $(Diso)_2Os(PPh_3) \bullet 2\ CH_2Cl_2$, with hydrogen atoms and solvent molecules omitted for clarity. Only the major orientation of the disordered *tert*-butyl group is shown.

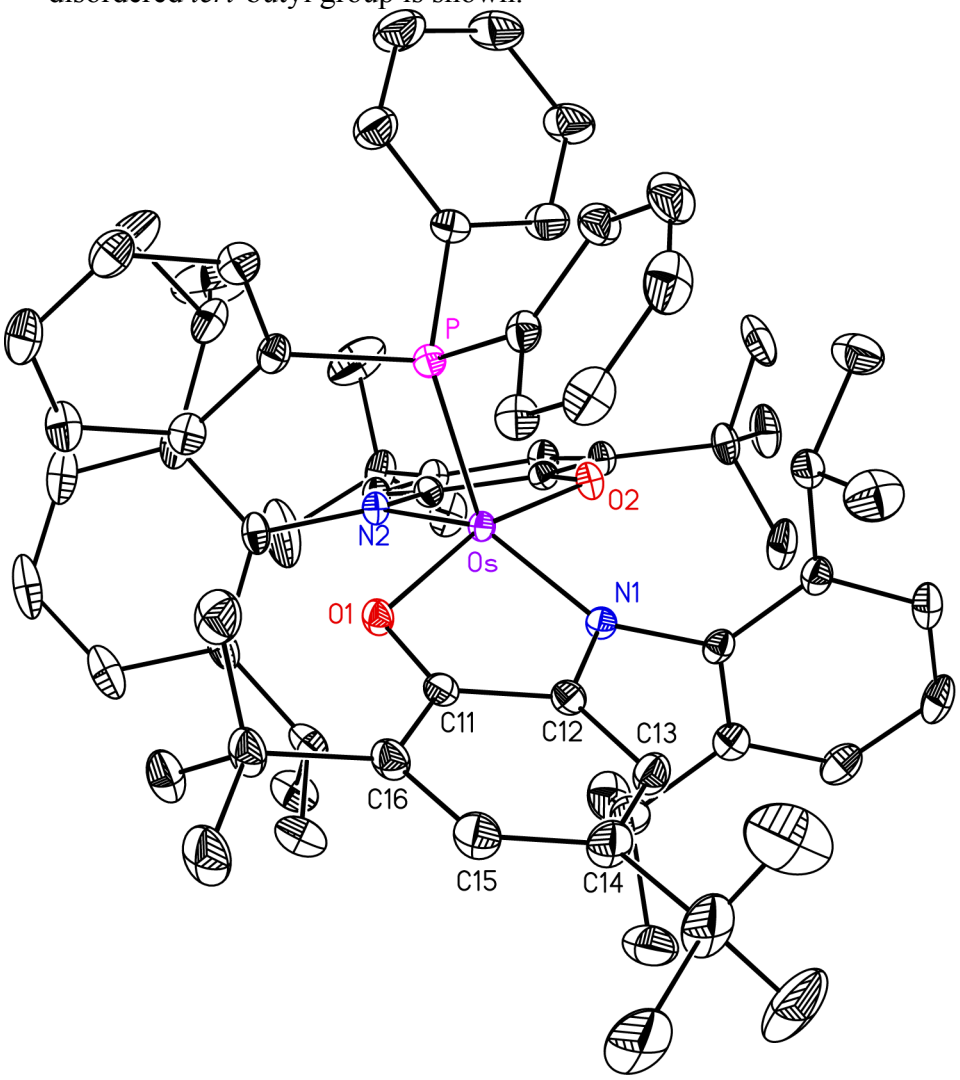

III. ^{1}H NMR spectra

Figure S6. ^{1}H NMR spectrum of *cis*-$(Diso)_2RuCl_2$ ($CDCl_3$, 400 MHz)

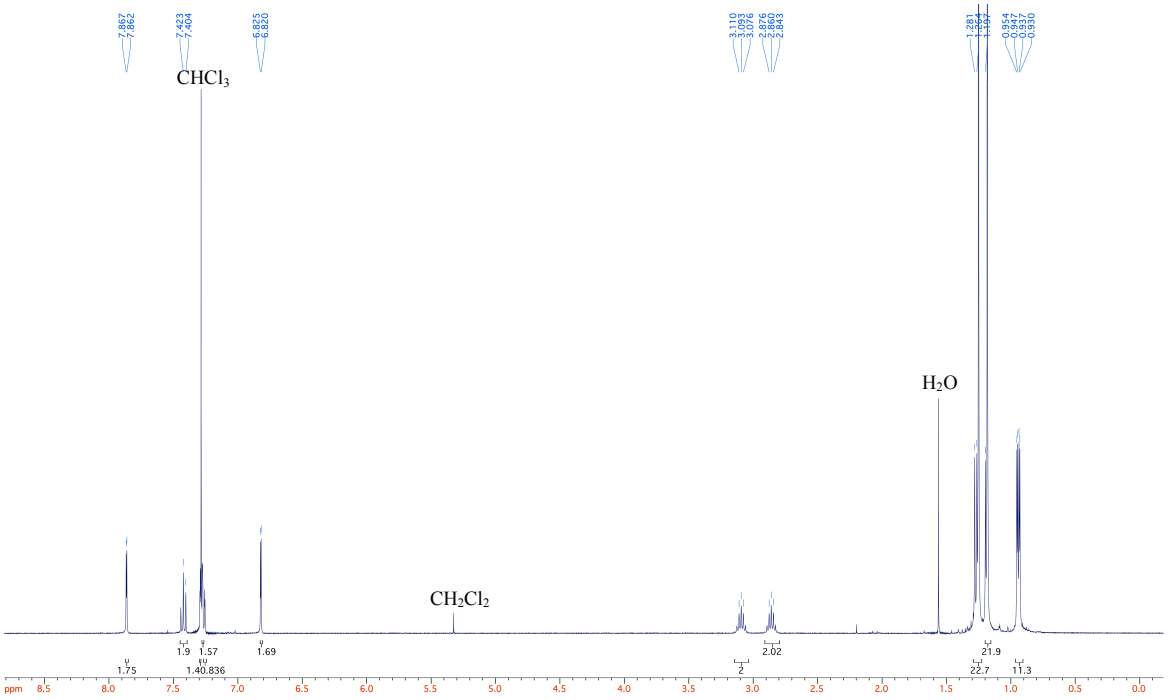

Figure S7. ^{1}H NMR spectrum of *trans*-$(Diso)_2RuCl_2$ ($CDCl_3$, 400 MHz)

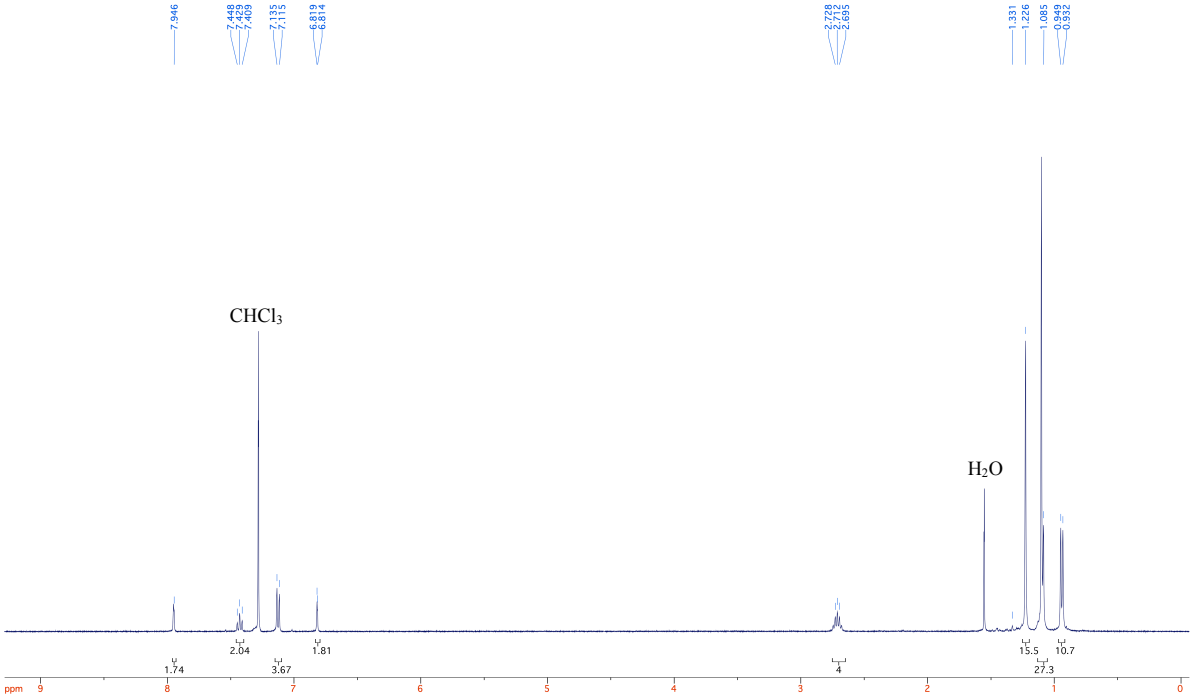

Figure S8. ^{1}H NMR spectrum of *cis*-(Diso)$_2$OsCl$_2$, (CD_2Cl_2, 400 MHz)

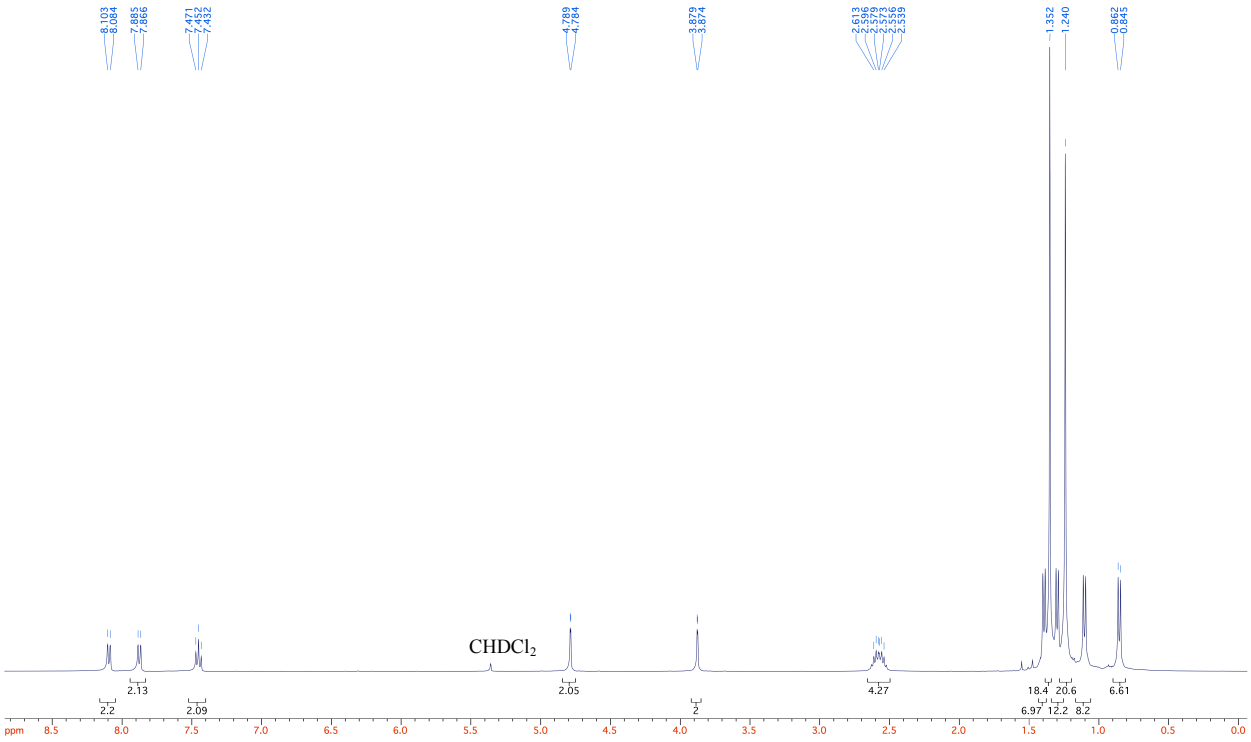

Figure S9. ^{1}H NMR spectrum of *trans*-(Diso)$_2$OsCl$_2$. Signals due to paramagnetic impurities marked with **P**. (CD_2Cl_2, 400 MHz)

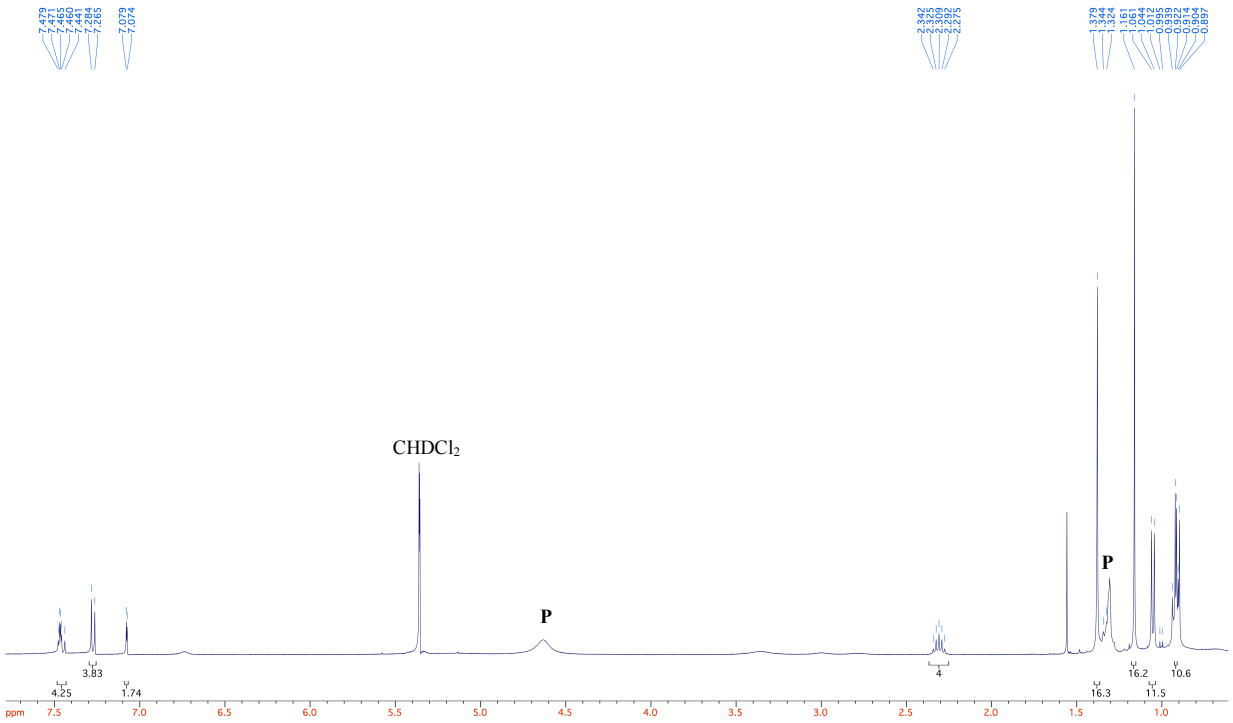

Figure S10. ^{1}H NMR spectrum of CF_3Tio ($CDCl_3$, 400 MHz)

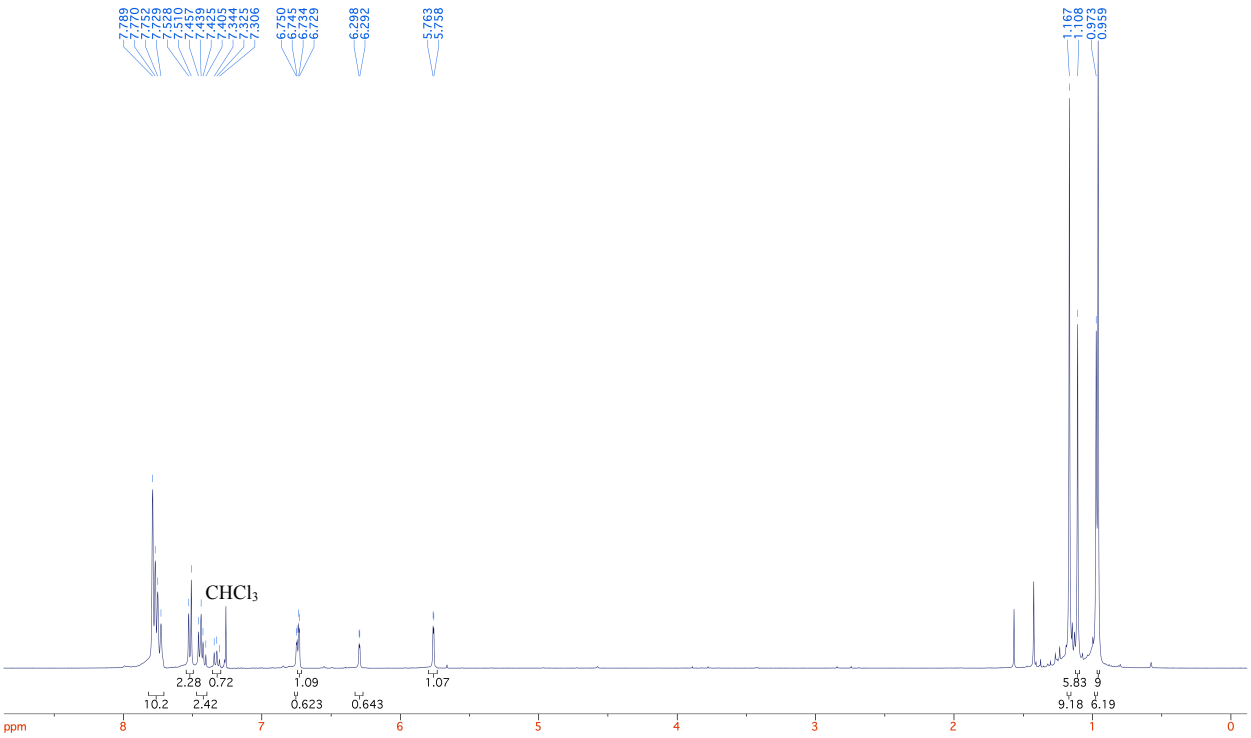

Figure S11. ^{1}H NMR spectrum of *trans*-$(CF_3Tio)_2RuCl_2$ (CD_2Cl_2, 400 MHz)

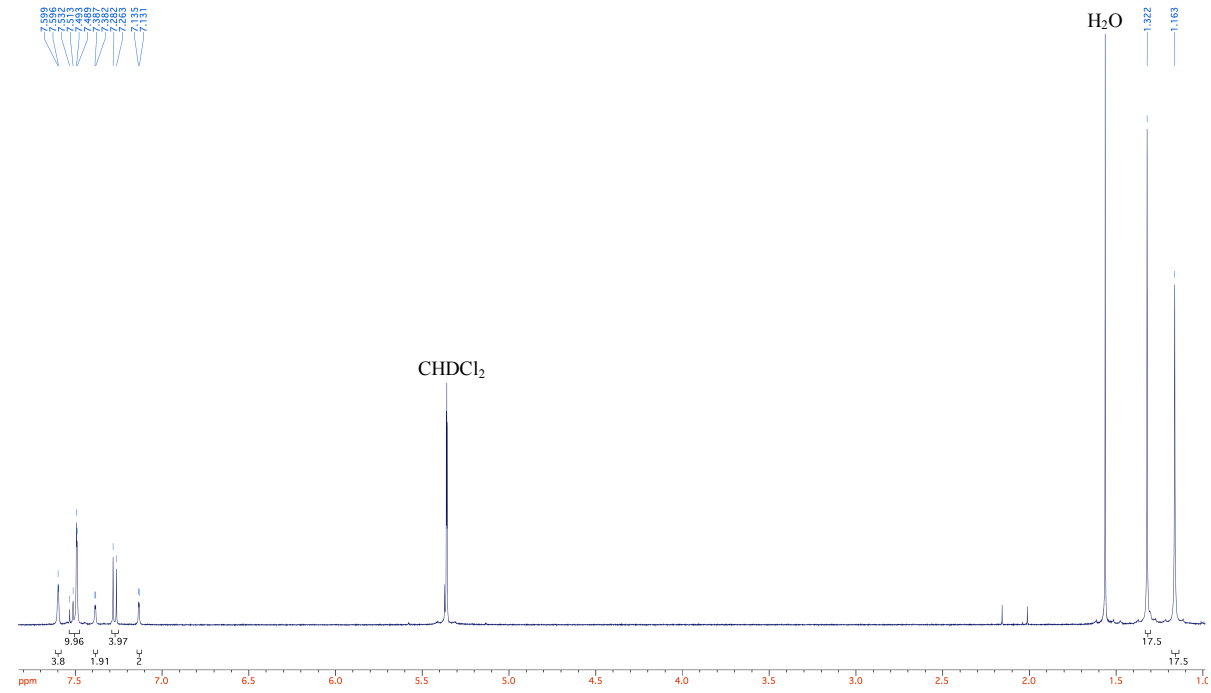

Figure S12. ^{1}H NMR spectrum of *cis*-$(CF_3Tio)_2RuCl_2$ (contaminated with 20% of the trans isomer). Peaks due to *trans*-$(CF_3Tio)_2RuCl_2$ marked with *. (CD_2Cl_2, 400 MHz)

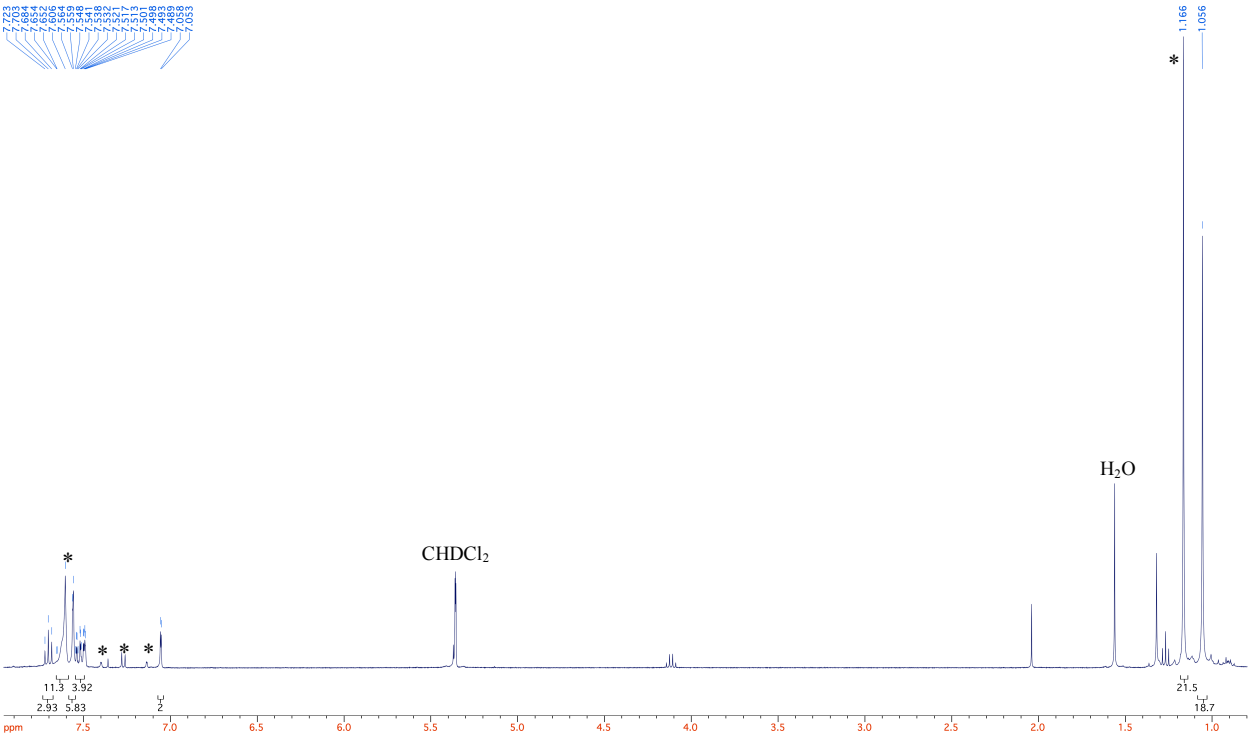

Figure S13. ^{1}H NMR spectrum of $(Diso)_2Ru(PPh_3)$ (CD_2Cl_2, –65 °C, 400 MHz)

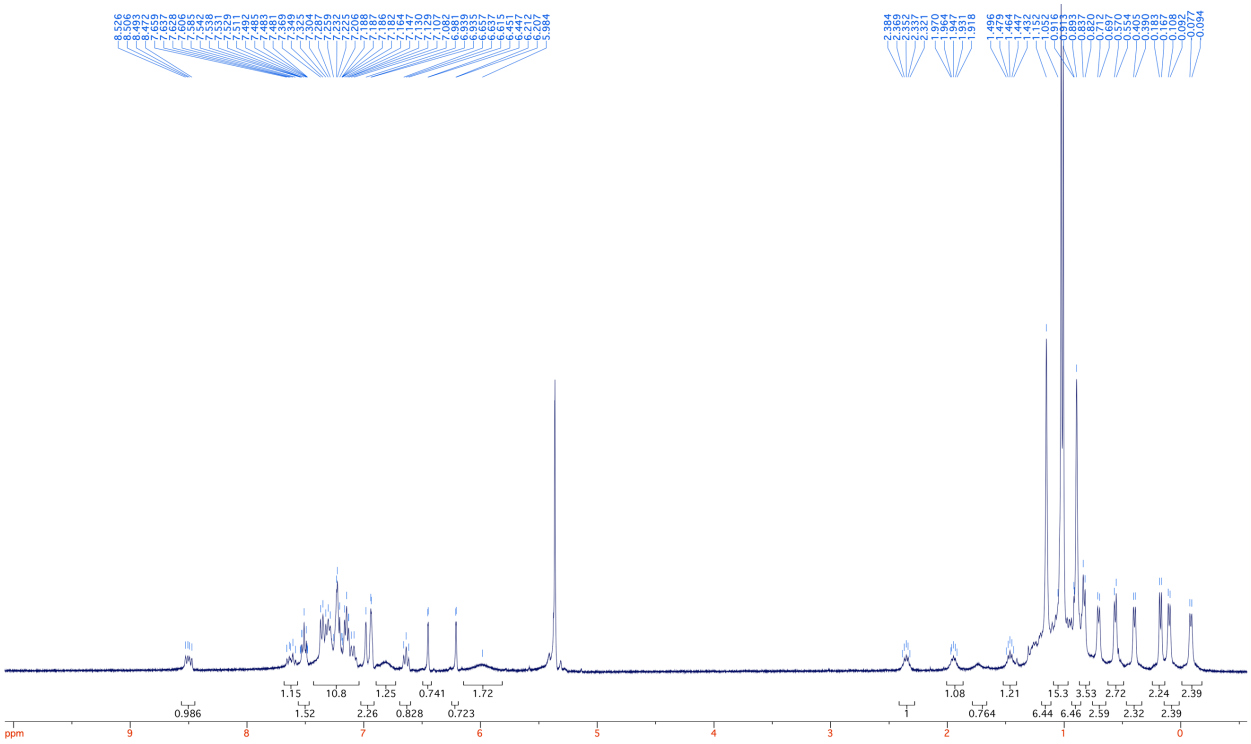

Figure S14. ^{1}H NMR spectrum of $(Diso)_2Os(PPh_3)$ (CD_2Cl_2, –78 °C, 400 MHz)

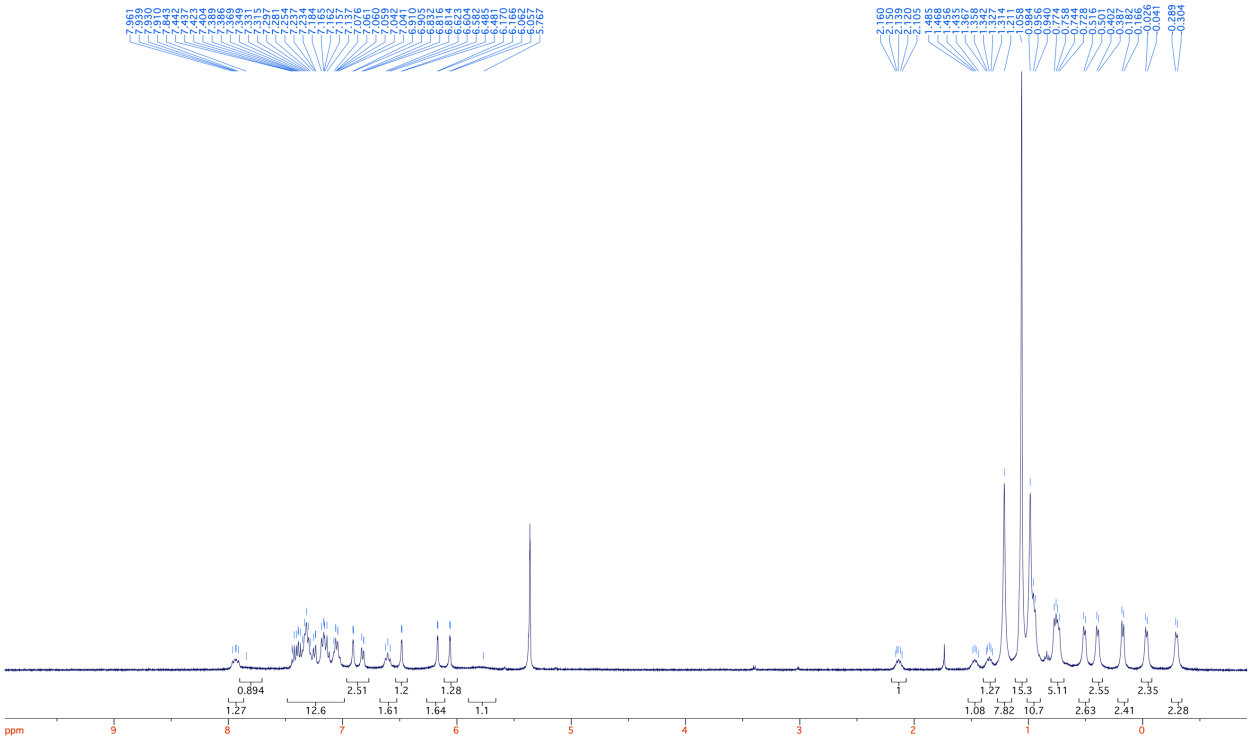

IV. $^{13}C\{^{1}H\}$ NMR spectra

Figure S15. $^{13}C\{^{1}H\}$ NMR spectrum of *cis*-$(Diso)_2RuCl_2$ ($CDCl_3$, 100.58 MHz)

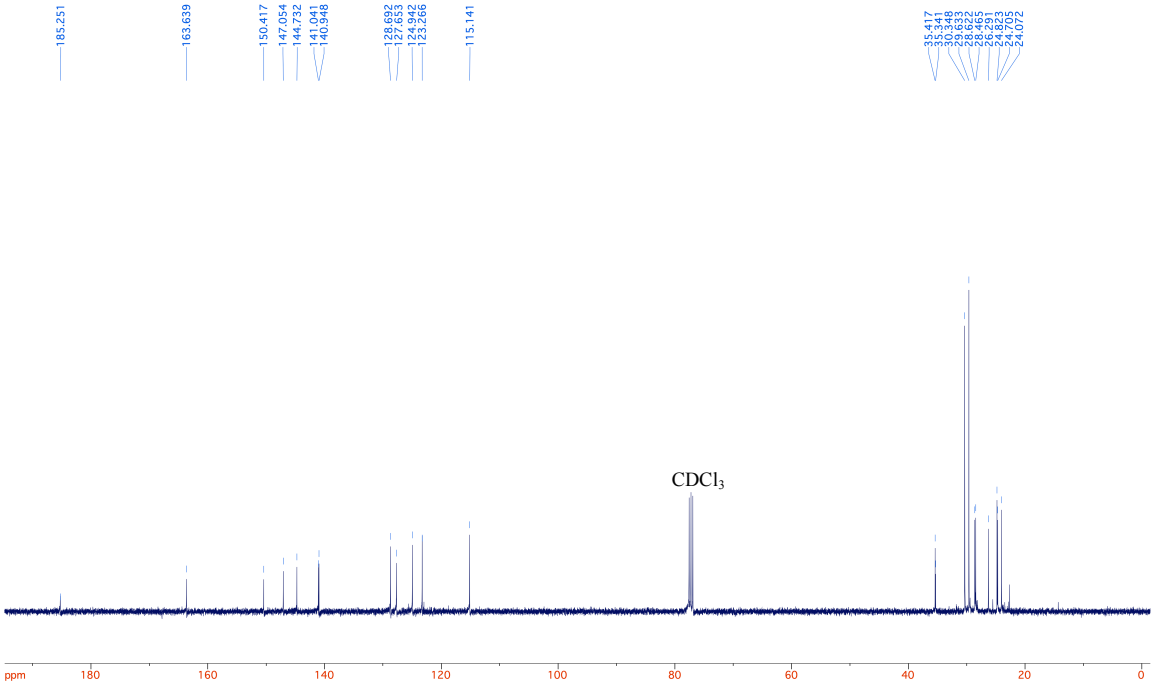

Figure S16. $^{13}C\{^{1}H\}$ NMR spectrum of *trans*-$(Diso)_2RuCl_2$ (CD_2Cl_2, 100.58 MHz)

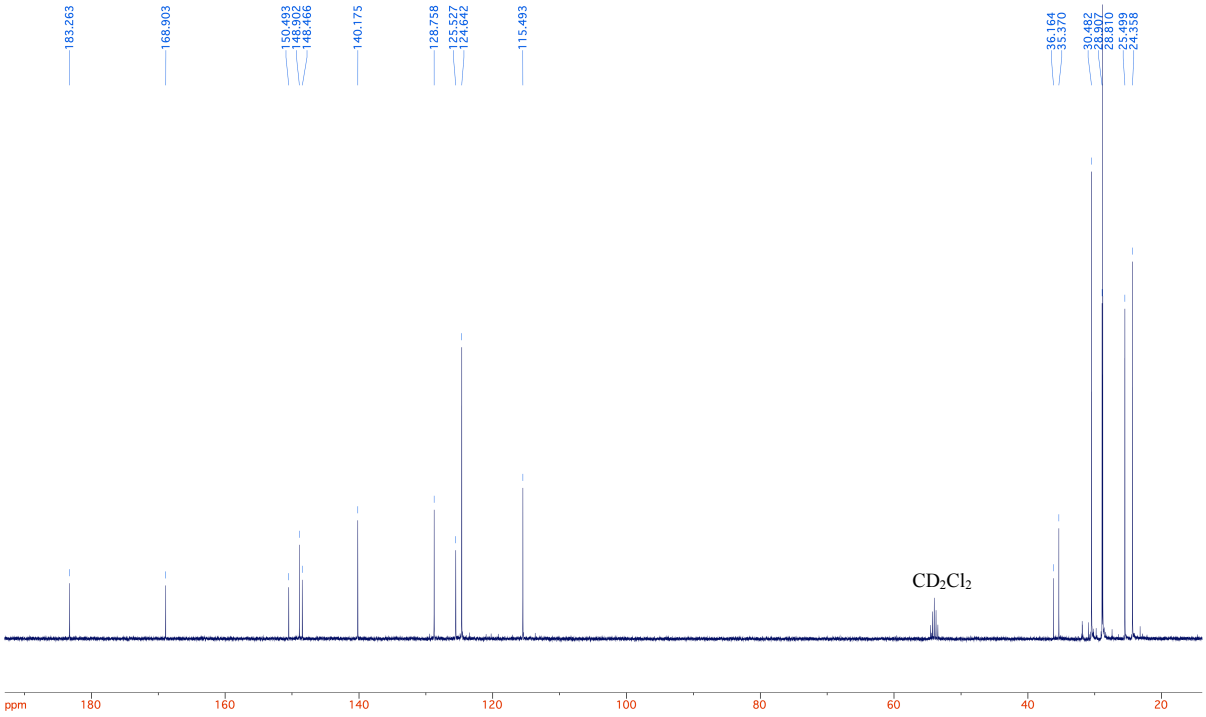

Figure S17. $^{13}C\{^{1}H\}$ NMR spectrum of *cis*-$(Diso)_2OsCl_2$ (CD_2Cl_2, 100.58 MHz)

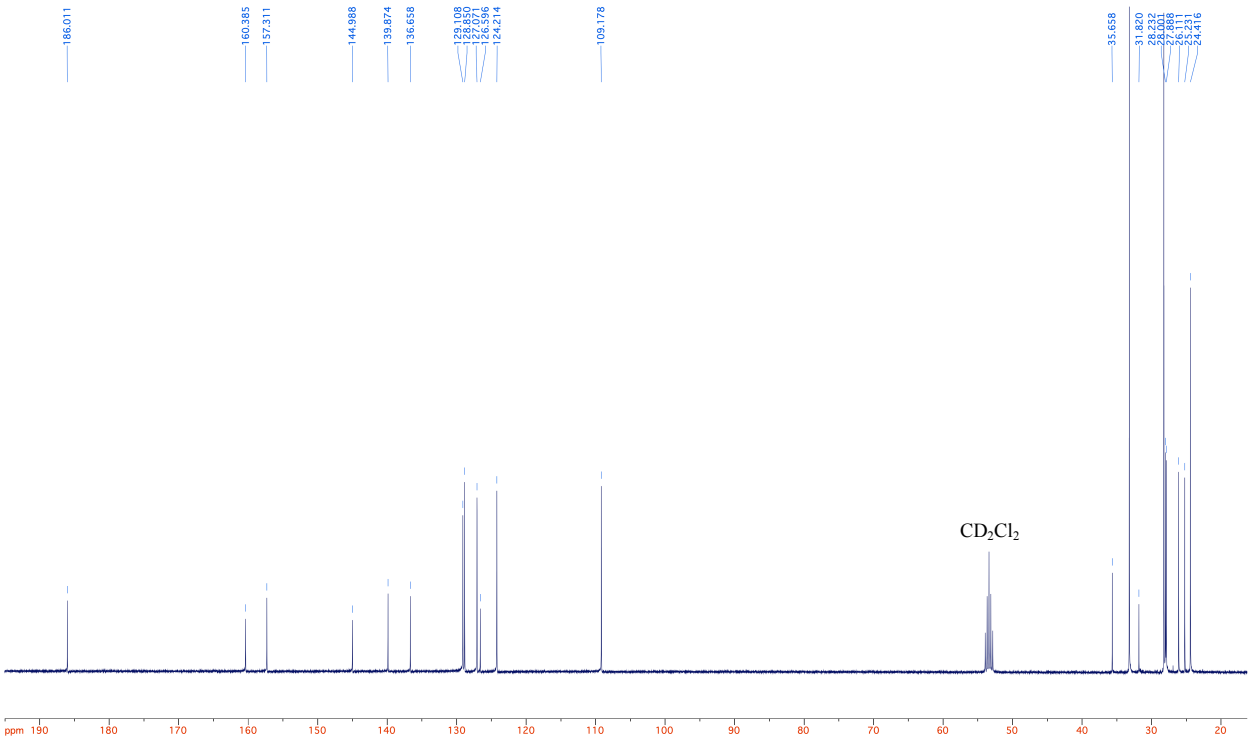

Figure S18. $^{13}C\{^{1}H\}$ NMR spectrum of CF_3Tio ($CDCl_3$, 100.58 MHz)

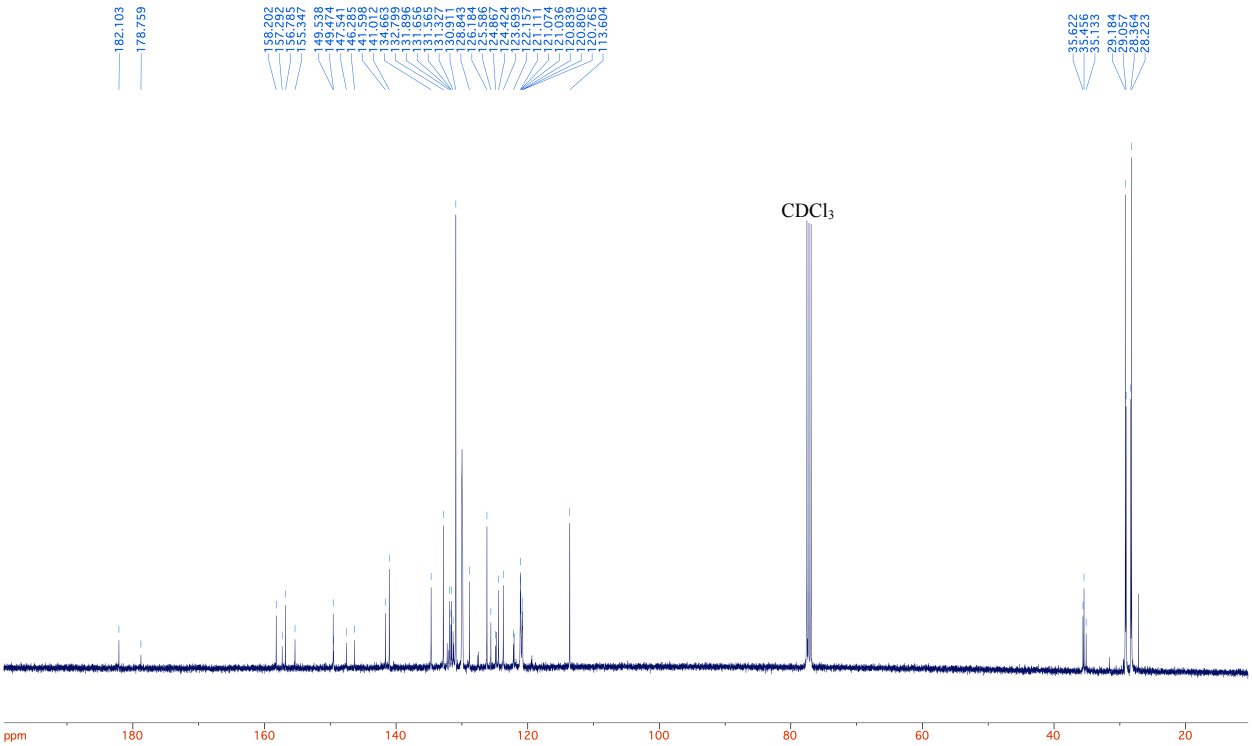

Figure S19. $^{13}C\{^{1}H\}$ NMR spectrum of 80:20 *cis*-/*trans*-$(CF_3Tio)_2RuCl_2$ mixture (CD_2Cl_2, 100.58 MHz)

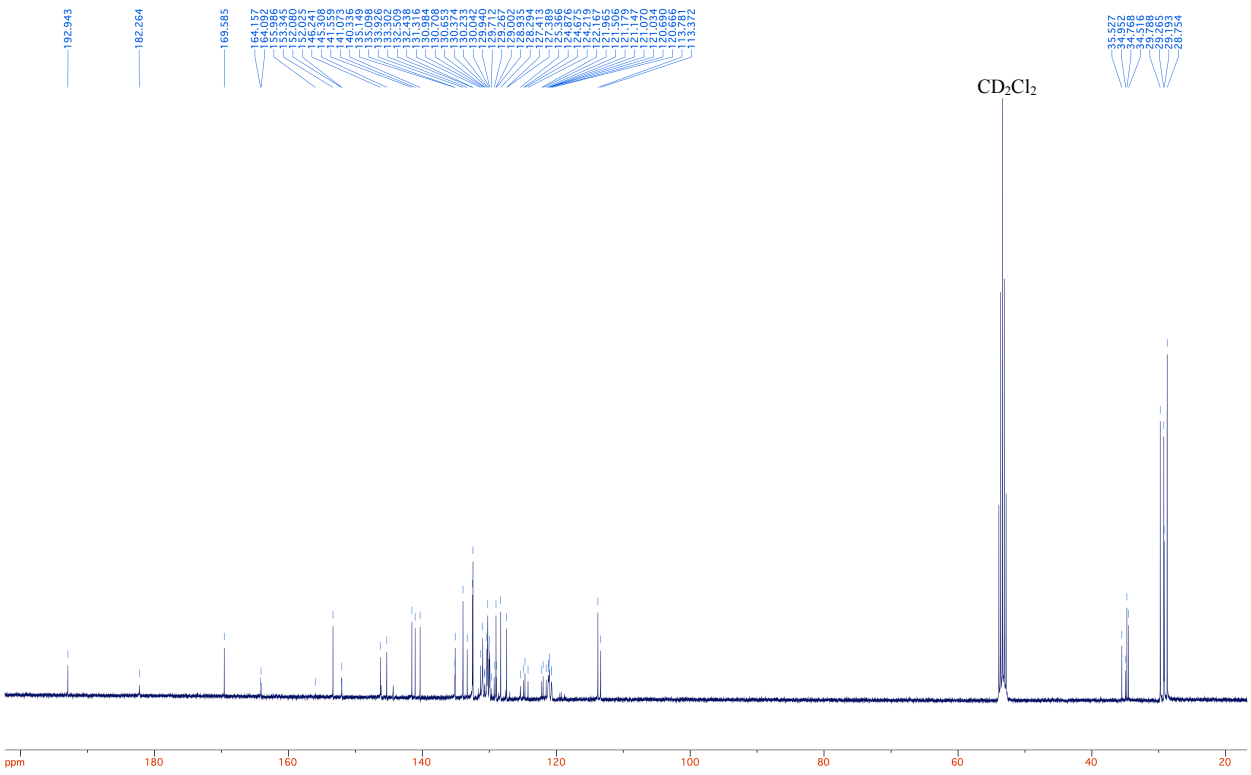

V. $^{19}F\{^{1}H\}$ NMR spectra

Figure S20. $^{19}F\{^{1}H\}$ NMR spectrum of CF_3Tio (CD_2Cl_2, 376.5 MHz)

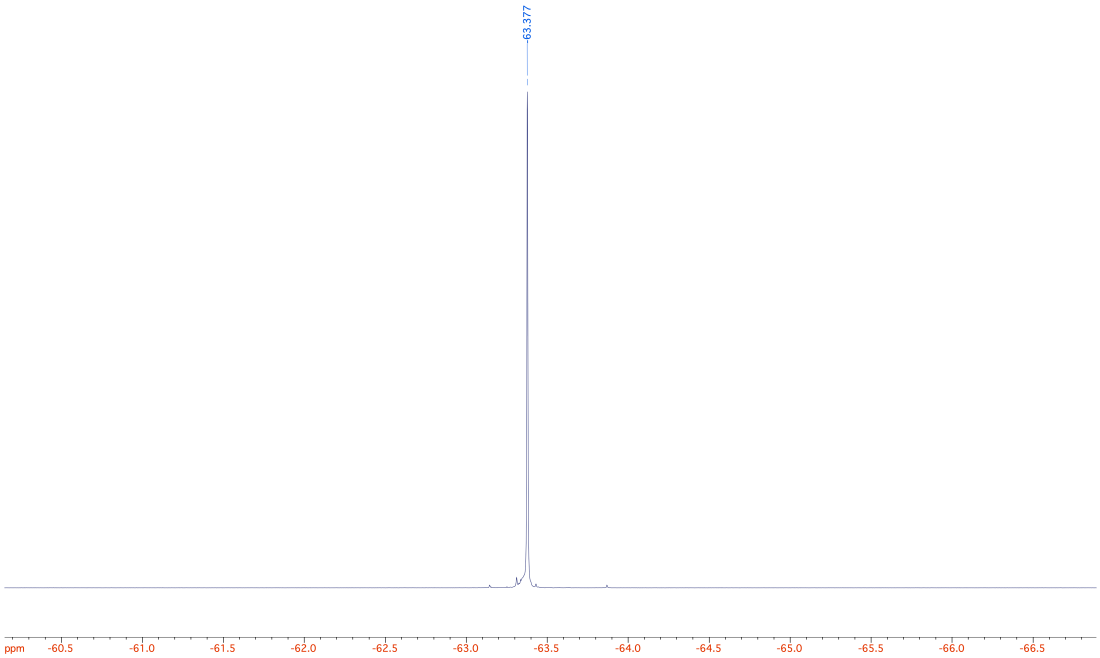

Figure S21. $^{19}F\{^{1}H\}$ NMR spectrum of *trans*-$(CF_3Tio)_2RuCl_2$ (CD_2Cl_2, 376.5 MHz)

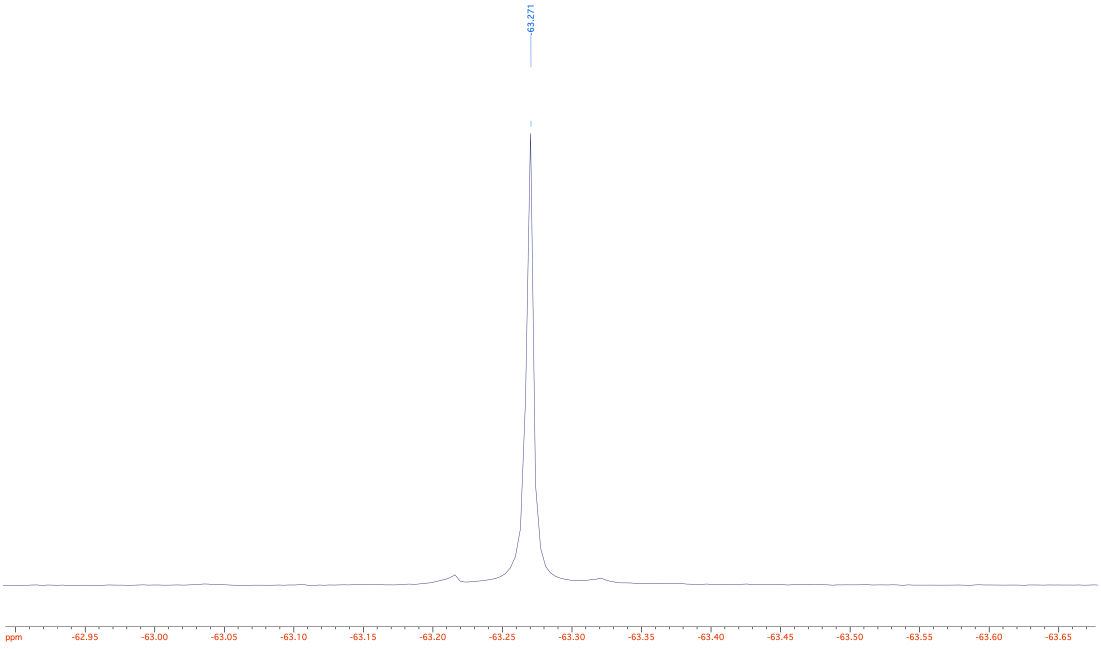

Figure S22. $^{19}F\{^{1}H\}$ NMR spectrum of 80:20 *cis*-/*trans*-$(CF_3Tio)_2RuCl_2$ mixture (CD_2Cl_2, 376.5 MHz)

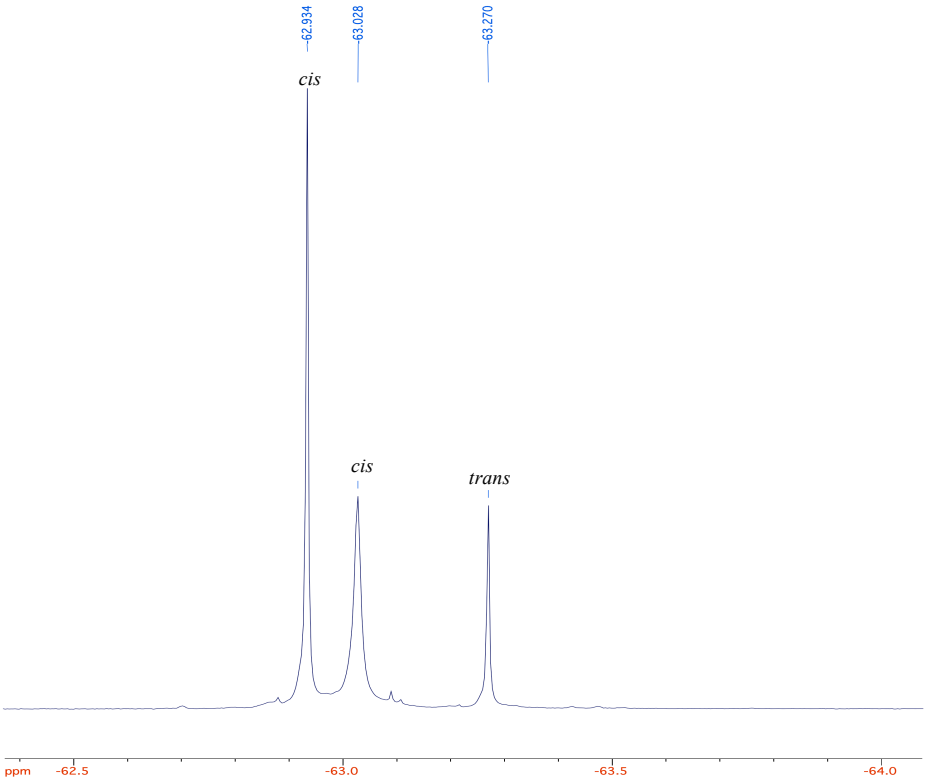

VI. $^{31}P\{^{1}H\}$ NMR spectra

Figure S23. $^{31}P\{^{1}H\}$ NMR spectrum of $(Diso)_2Ru(PPh_3)$ (CD_2Cl_2, 162.0 MHz)

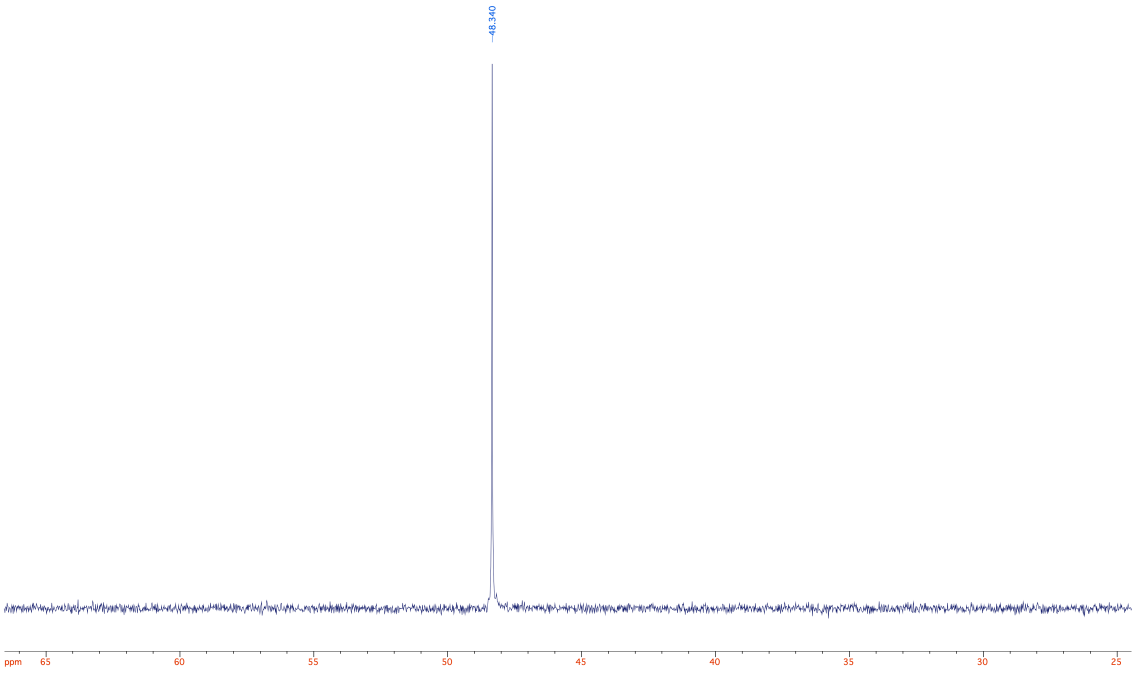

Figure S24. $^{31}P\{^{1}H\}$ NMR spectrum of $(Diso)_2Os(PPh_3)$ (CD_2Cl_2, 162.0 MHz)

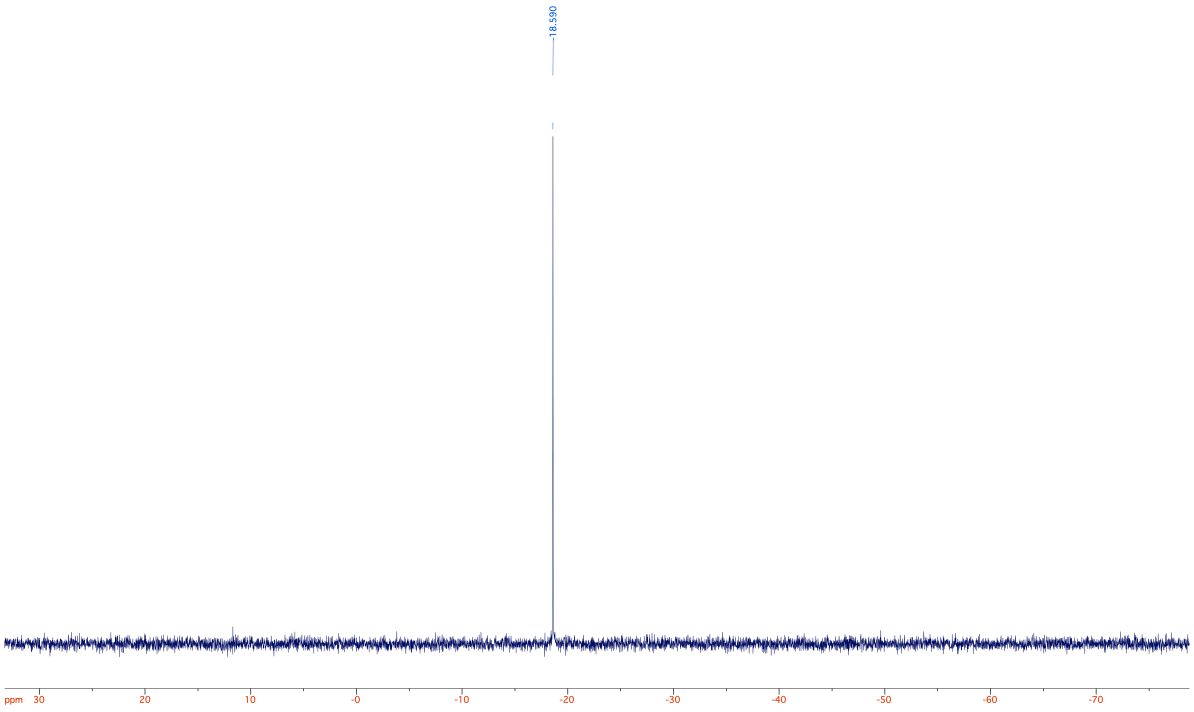

VII. Infrared spectra

Figure S25. Infrared spectrum of *cis*-$(Diso)_2RuCl_2$ (ATR)

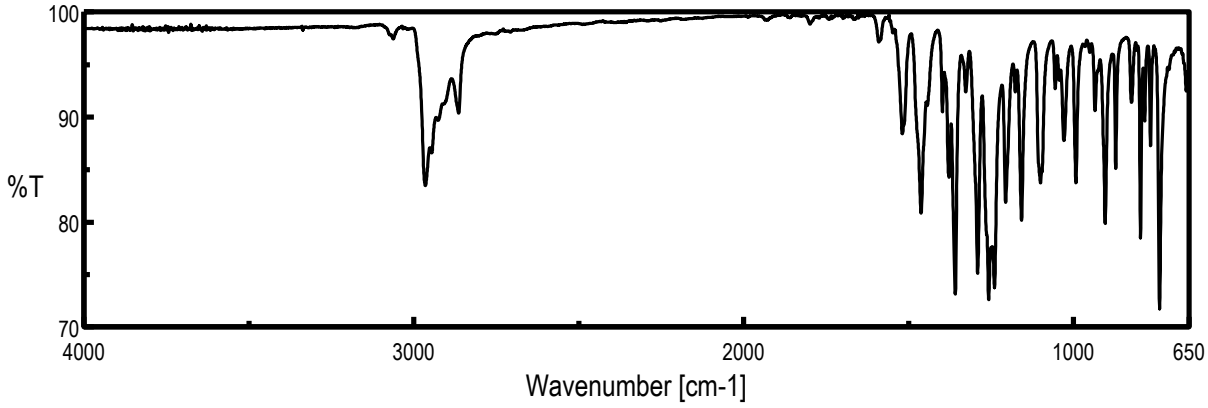

Figure S26. Infrared spectrum of *trans*-$(Diso)_2RuCl_2$ (ATR)

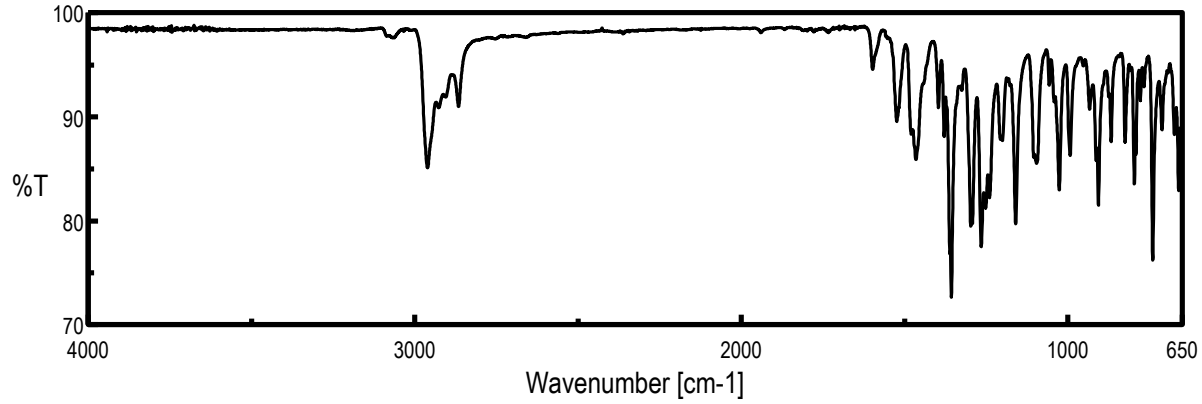

Figure S27. Infrared spectrum of *cis*-$(Diso)_2OsCl_2$ (evapd film)

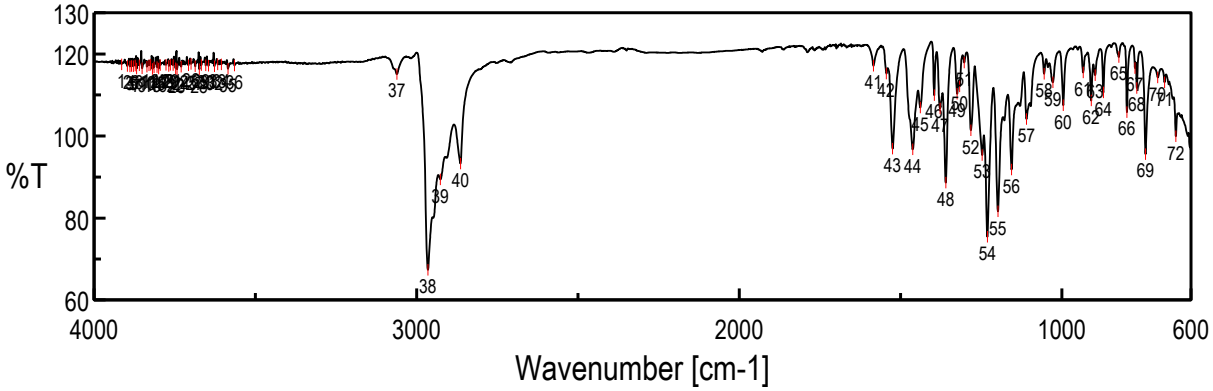

Figure S28. Infrared spectrum of CF_3Tio (evapd film)

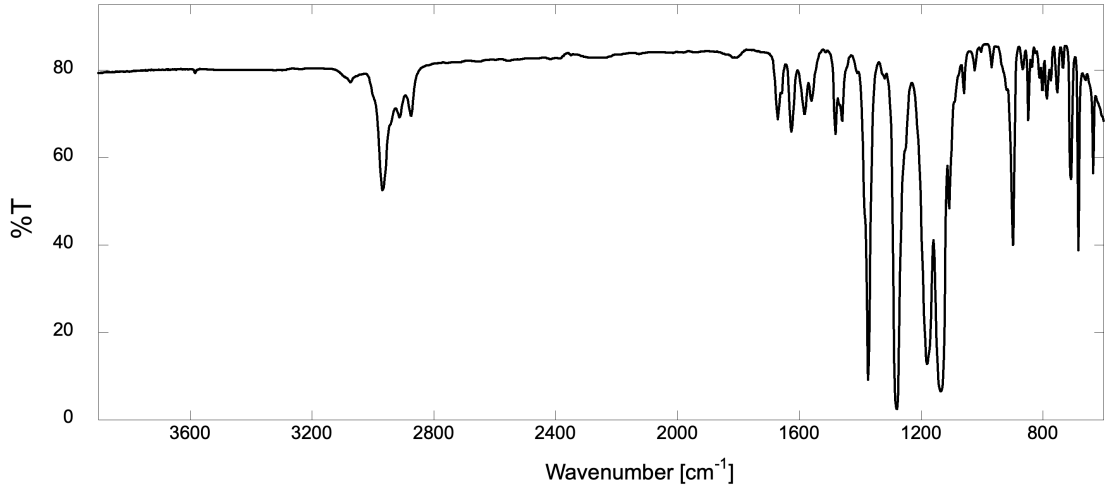

Figure S29. Infrared spectrum of *trans*-$(CF_3Tio)_2RuCl_2$ (ATR)

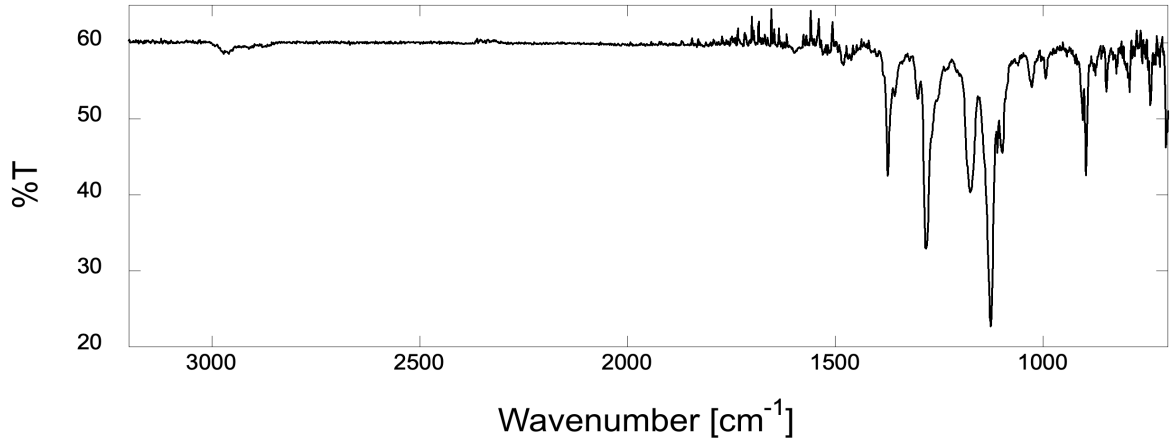

Figure S30. Infrared spectrum of 80:20 *cis*-/*trans*-$(CF_3Tio)_2RuCl_2$ mixture (evapd film)

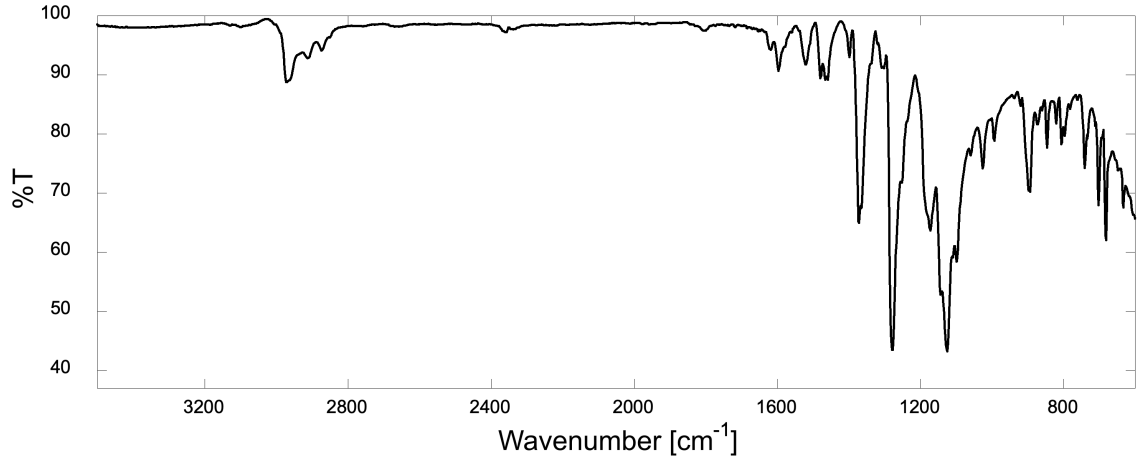

Figure S31. Infrared spectrum of $(Diso)_2Ru(PPh_3)$ (nujol mull)

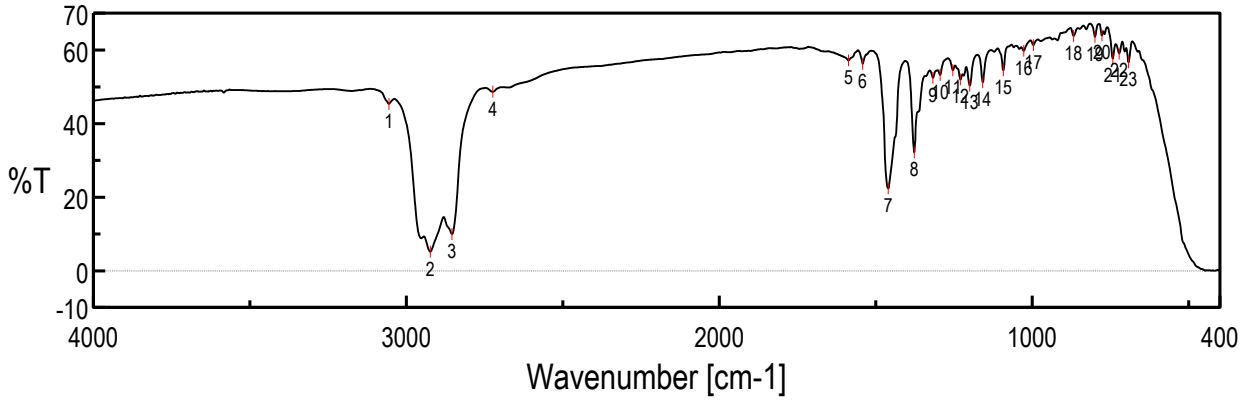

Figure S32. Infrared spectrum of $(Diso)_2Os(PPh_3)$ (nujol mull)

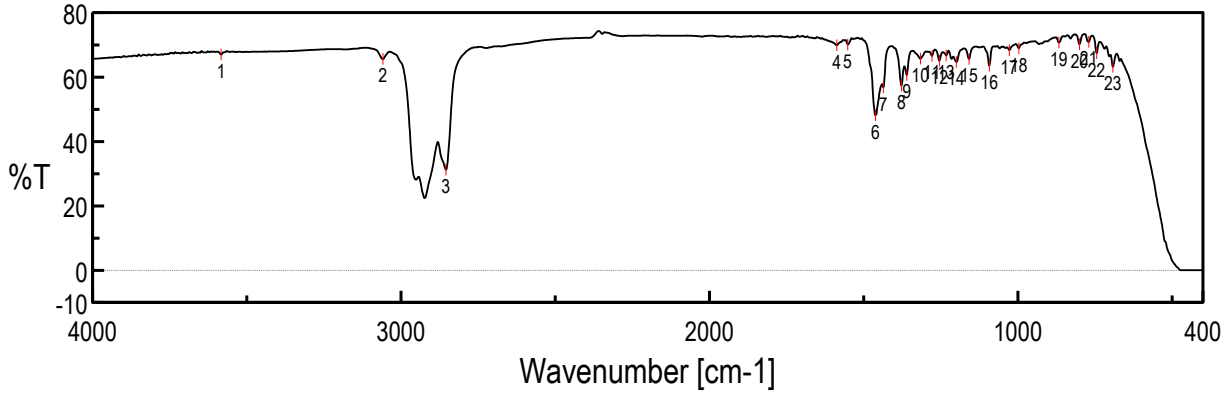

VIII. Optical Spectra

Figure S33. UV-Vis spectrum of *cis*-$(Diso)_2RuCl_2$ (CH_2Cl_2)

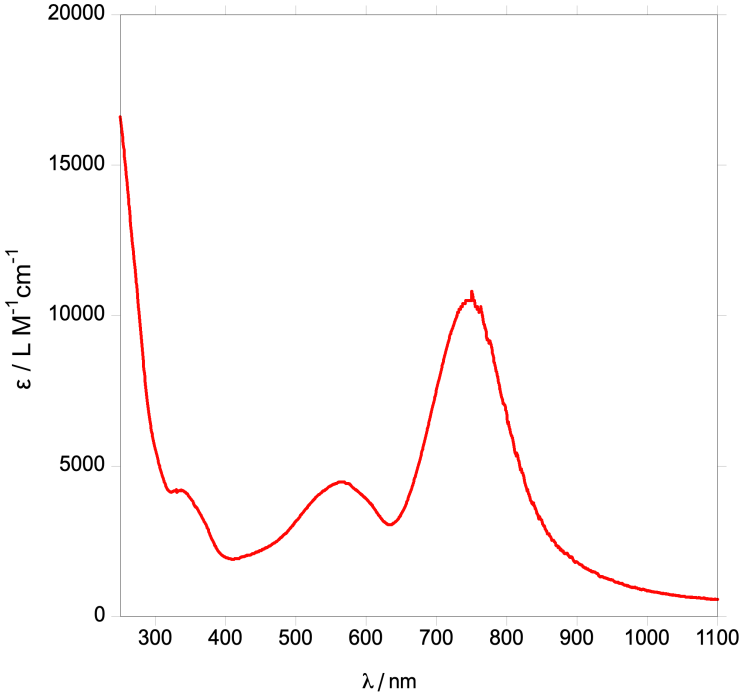

Figure S34. UV-Vis spectrum of *trans*-$(Diso)_2RuCl_2$ (CH_2Cl_2)

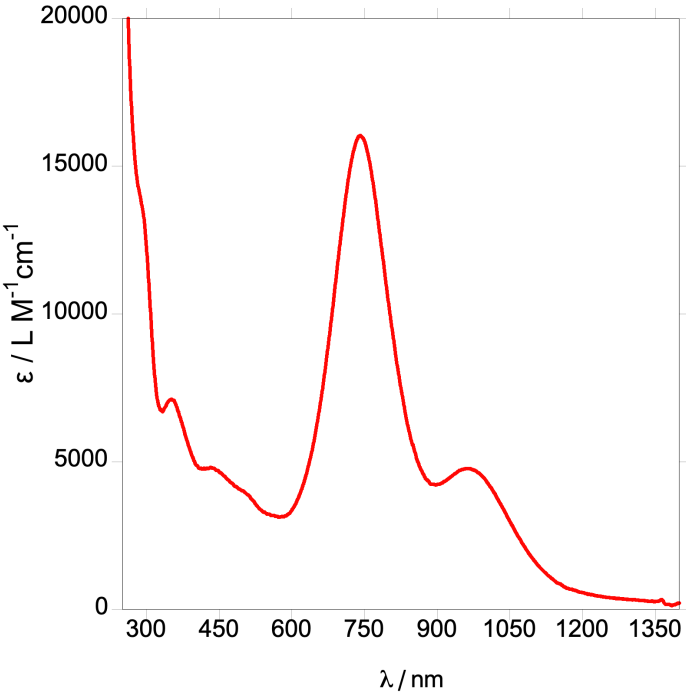

Figure S35. UV-Vis spectrum of *cis*-$(Diso)_2OsCl_2$ (CH_2Cl_2)

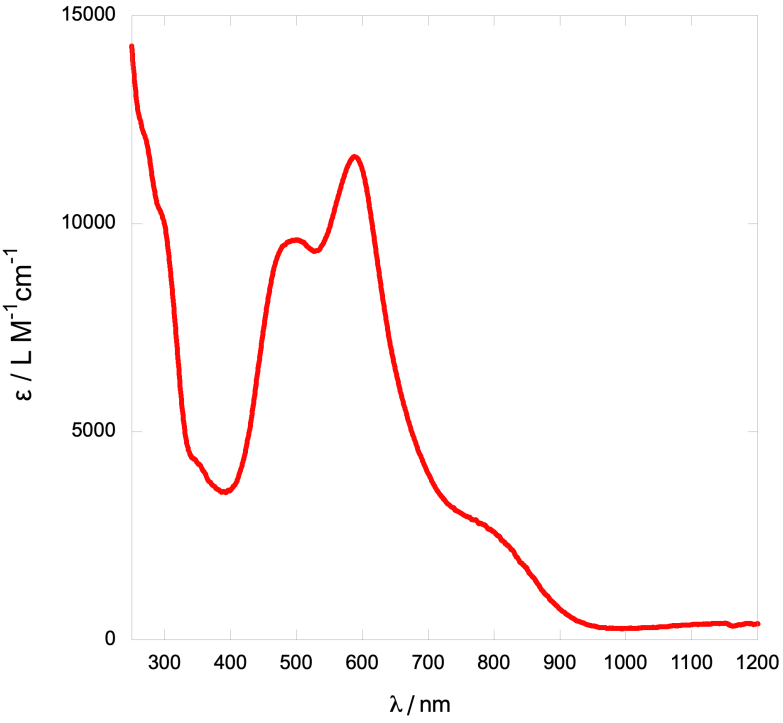

Figure S36. UV-Vis spectrum of CF_3Tio (CH_2Cl_2)

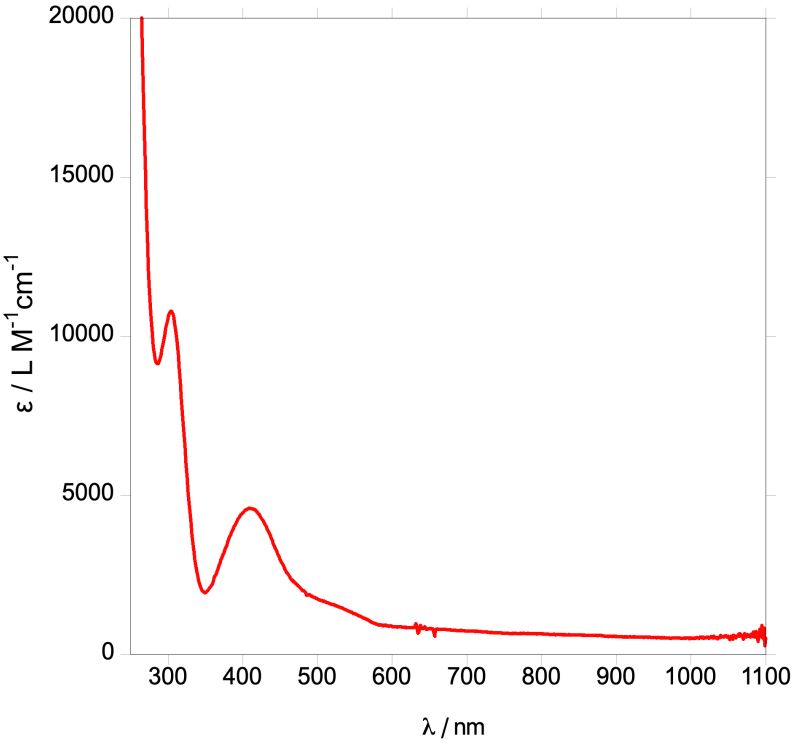

Figure S37. UV-Vis-NIR spectrum of *trans*-$(CF_3Tio)_2RuCl_2$ (CH_2Cl_2)

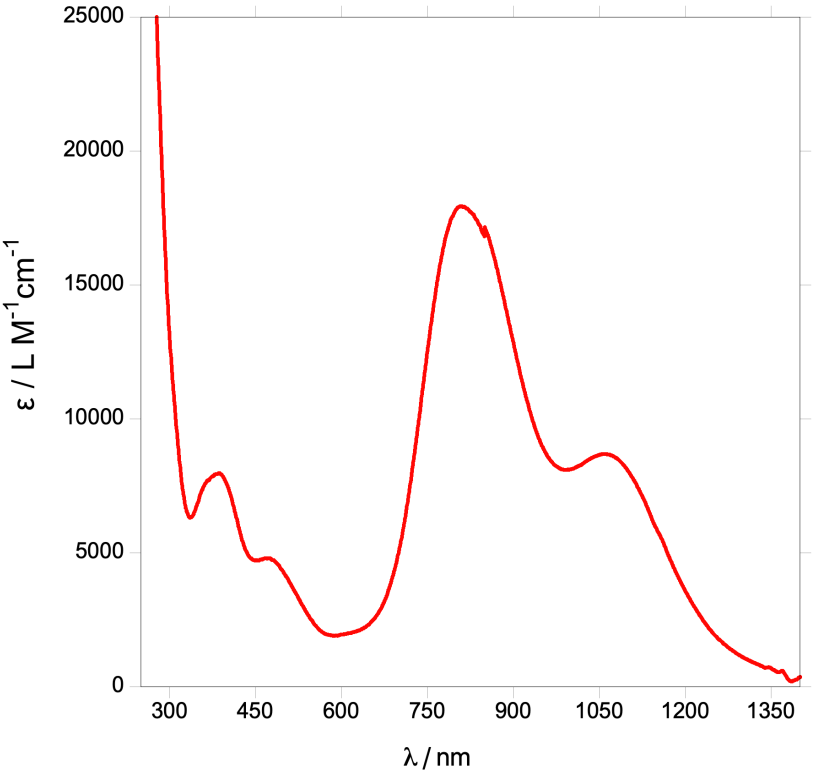

Figure S38. UV-Vis-NIR spectrum of *cis*- and *trans*-$(CF_3Tio)_2RuCl_2$ (CH_2Cl_2)

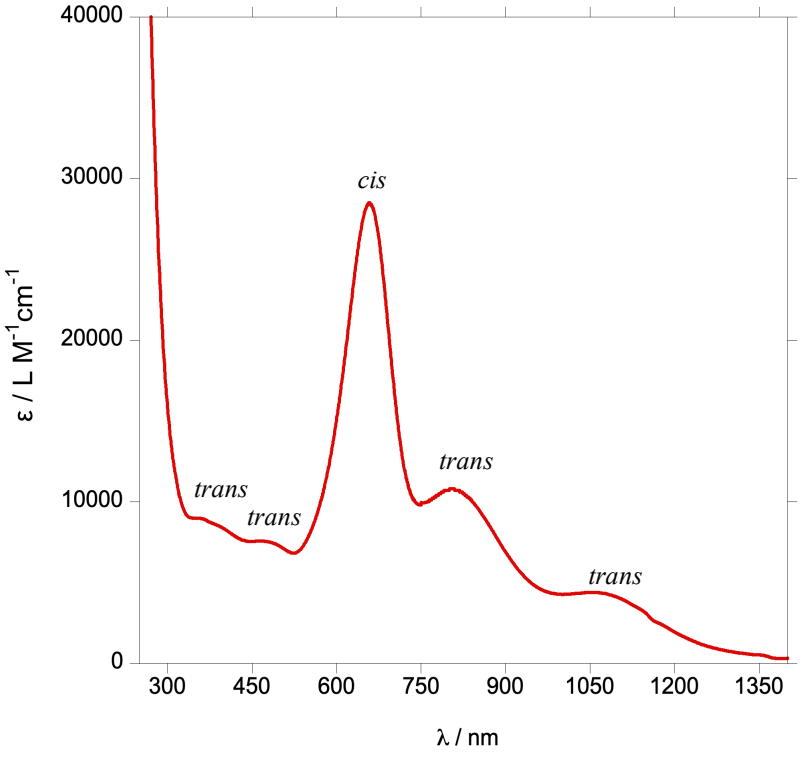

Figure S39. UV-Vis spectrum of $(Diso)_2Ru(PPh_3)$ (CH_2Cl_2)

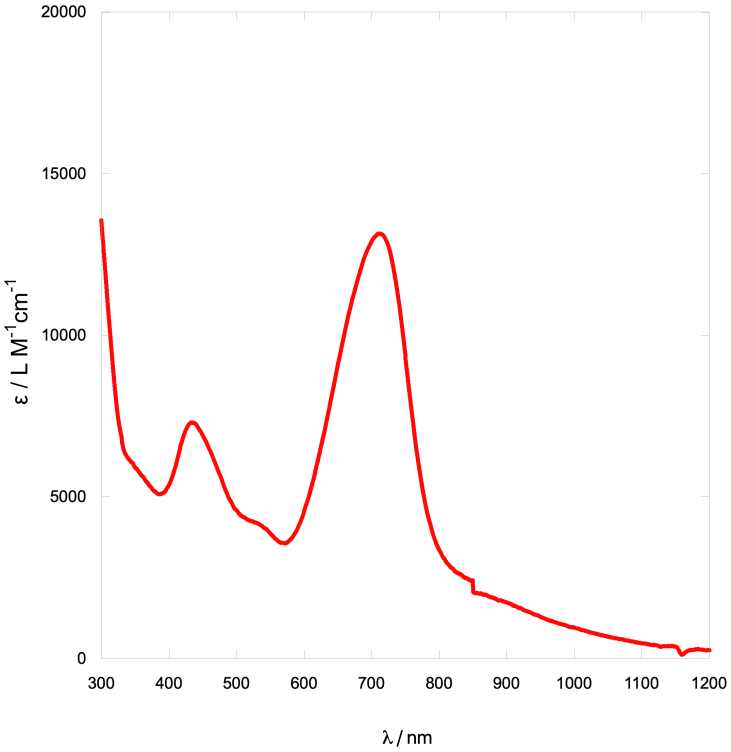

Figure S40. UV-Vis spectrum of $(Diso)_2Os(PPh_3)$ (CH_2Cl_2)

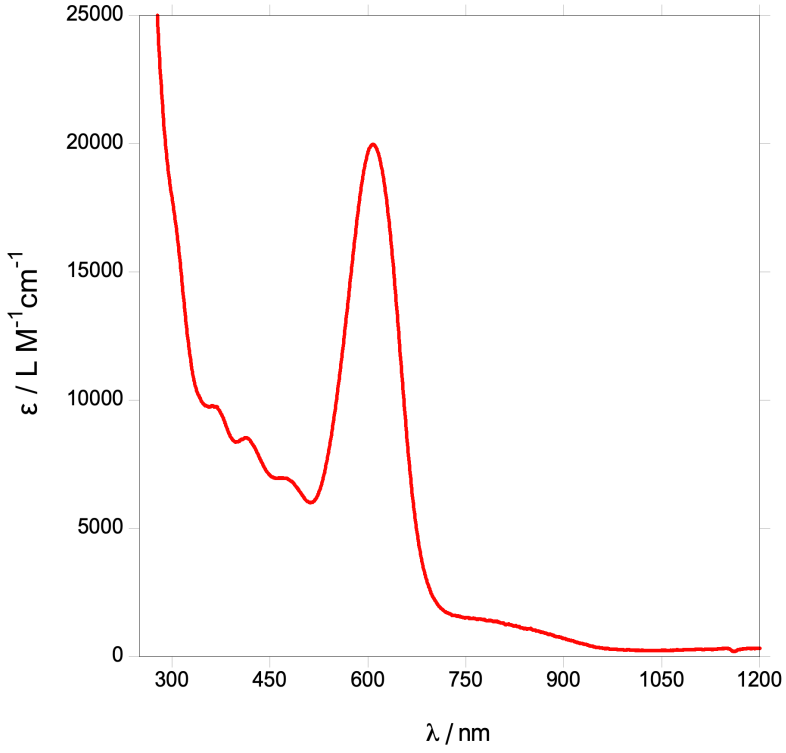

IX. Cyclic Voltammetry

Figure S41. CV of *cis*-$(Diso)_2RuCl_2$

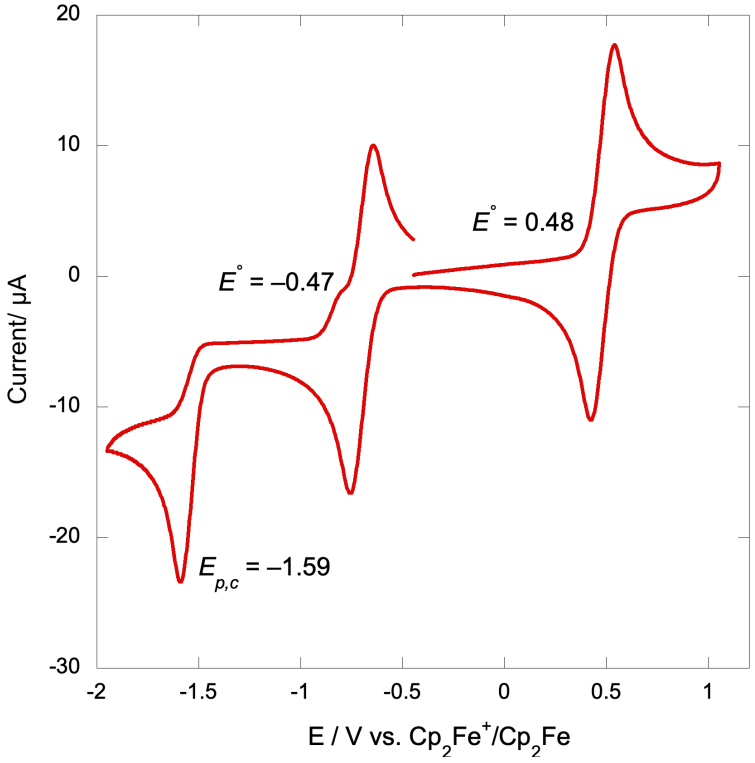

Figure S42. CV of *trans*-$(Diso)_2RuCl_2$

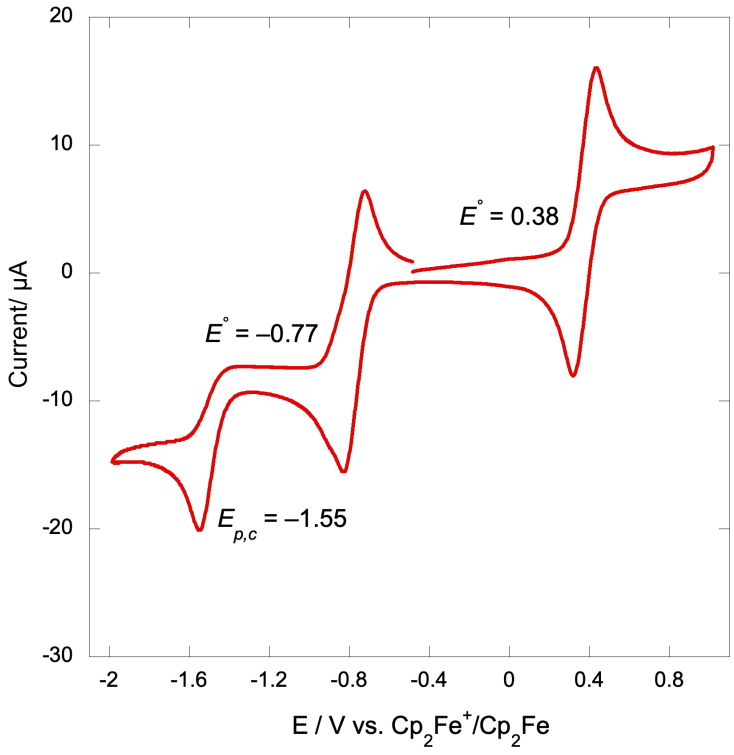

Figure S43. CV of *cis*-$(Diso)_2OsCl_2$

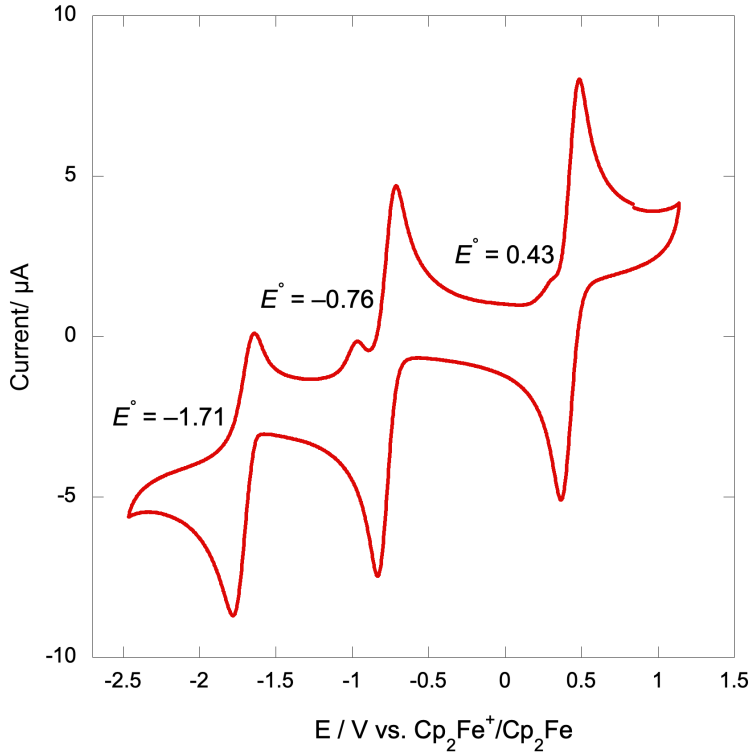

Figure S44. CV of $(Diso)_2Ru(PPh_3)$

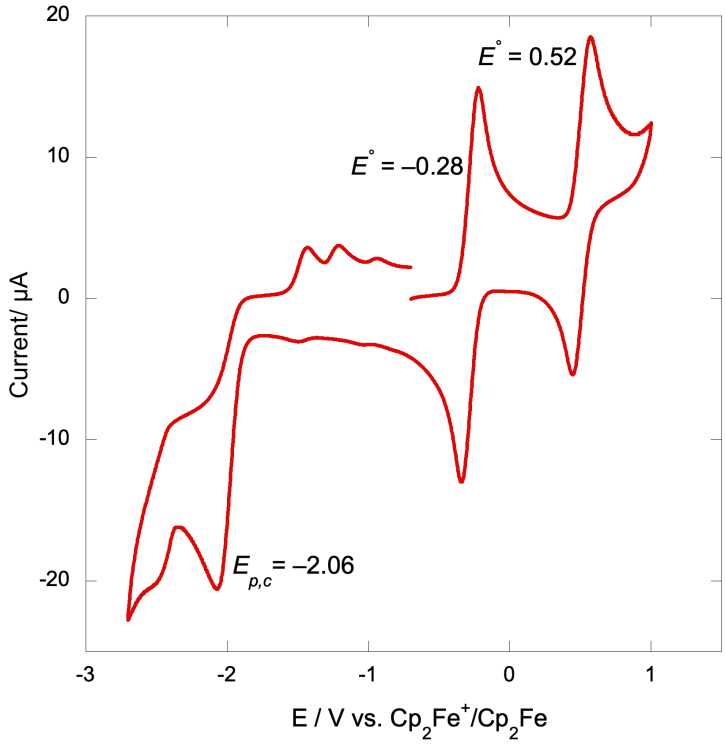

Figure S45. CV of $(Diso)_2Os(PPh_3)$

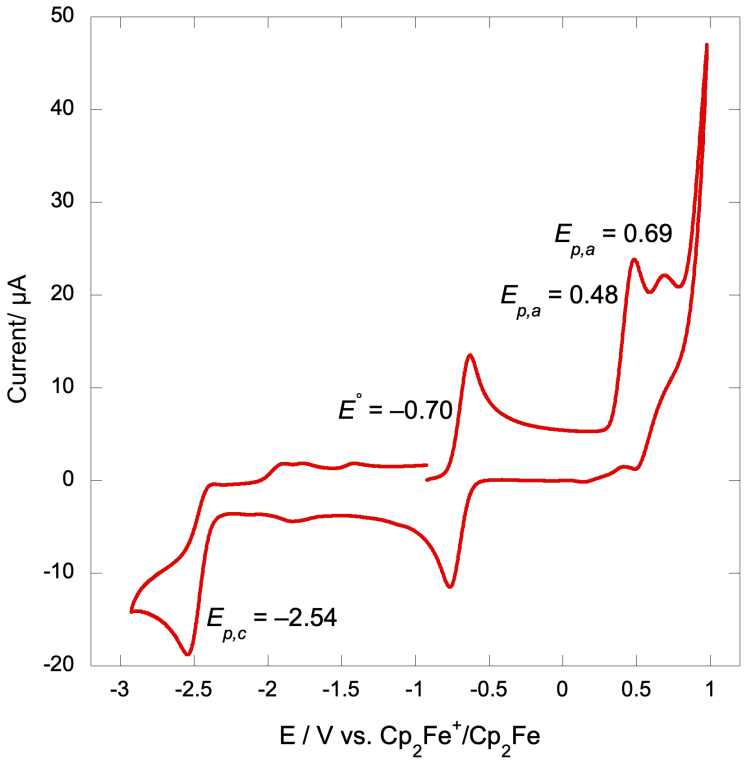

X. Variable-temperature NMR spectra

Figure S46. Variable-temperature ^{1}H NMR of *trans*-$(Diso)_2RuCl_2$ (80:20 CF_2Cl_2: $CDFCl_2$, 400 MHz)

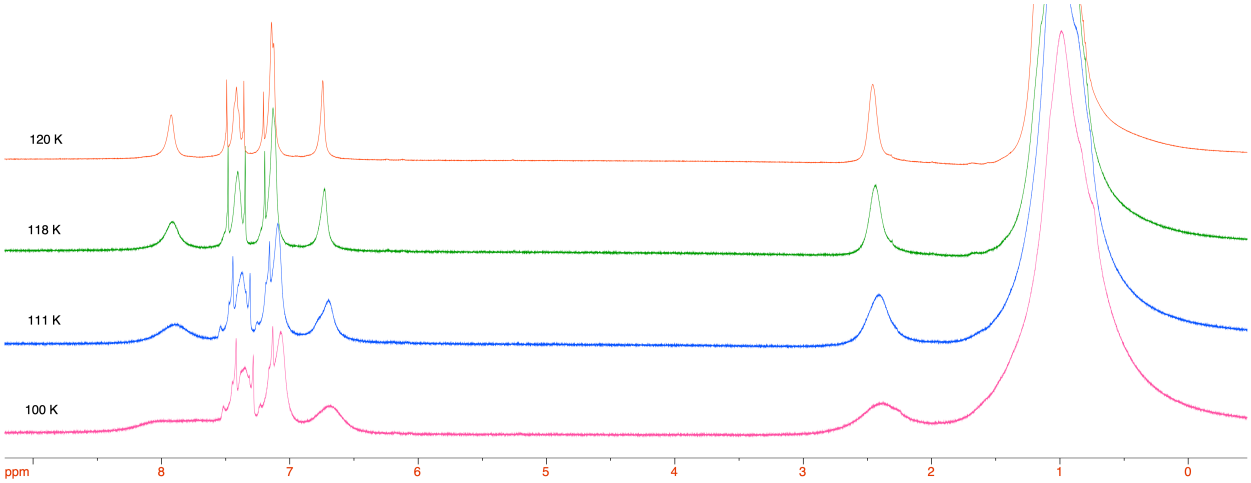

Figure S47. Variable-temperature ^{1}H NMR of *trans*-$(Diso)_2OsCl_2$ (80:20 CF_2Cl_2:$CDFCl_2$, 400 MHz)

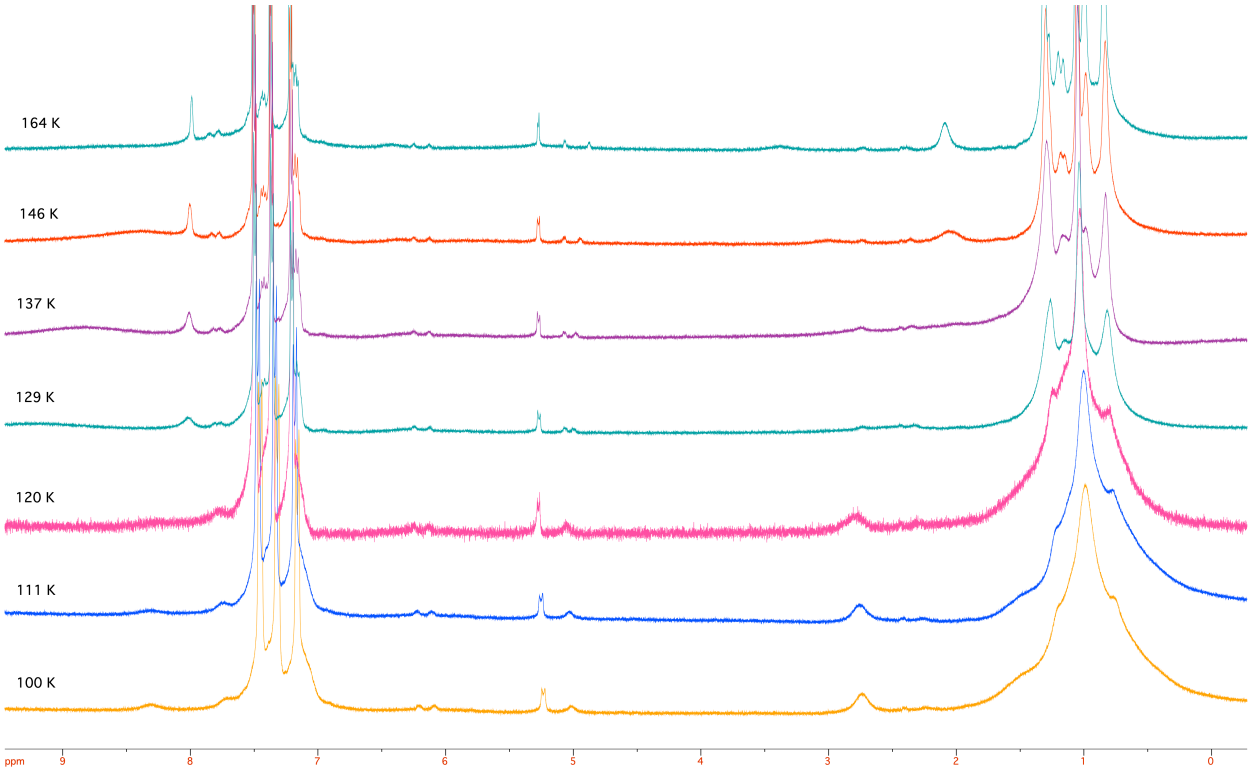

Figure S48. Variable-temperature ^{1}H NMR of $(Diso)_2Ru(PPh_3)$ (toluene-d_8, 400 MHz)

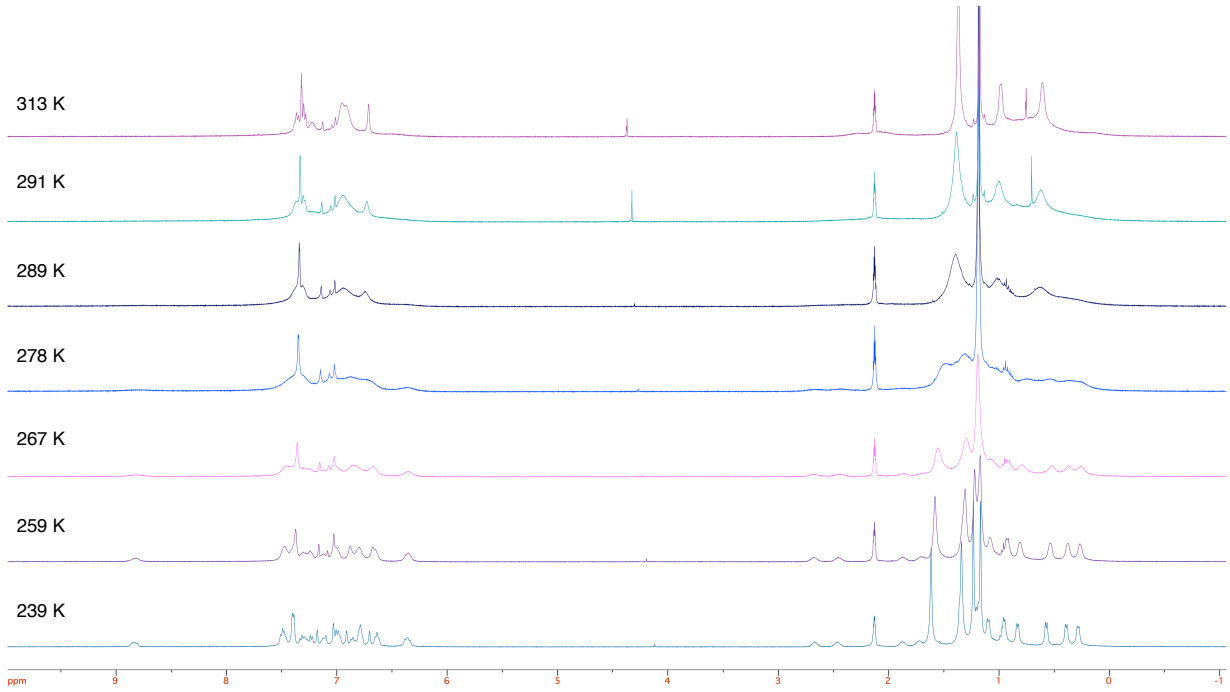

Figure S49. Variable-temperature ^{1}H NMR of $(Diso)_2Os(PPh_3)$ (toluene-d_8, 400 MHz)

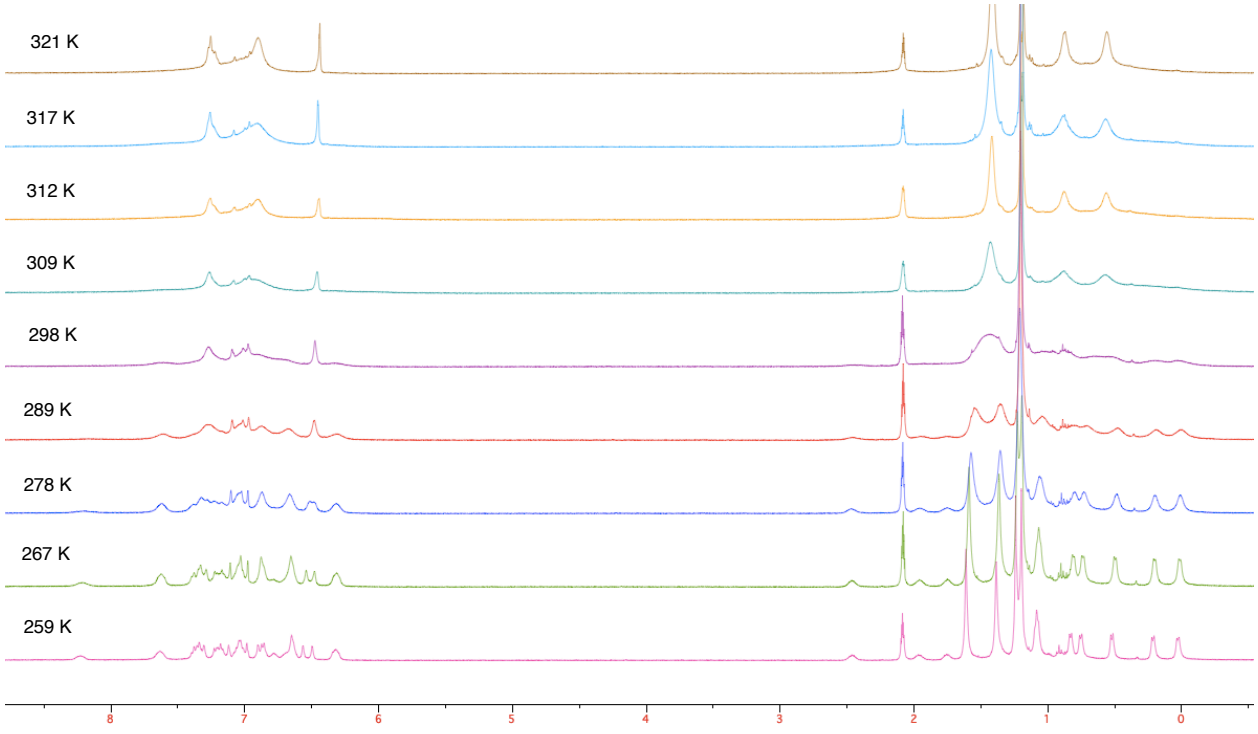

Figure S50. Eyring Plot for dynamics in *trans*-$(Diso)_2RuCl_2$ (red circles) and *trans*-$(Diso)_2OsCl_2$ (blue circles).

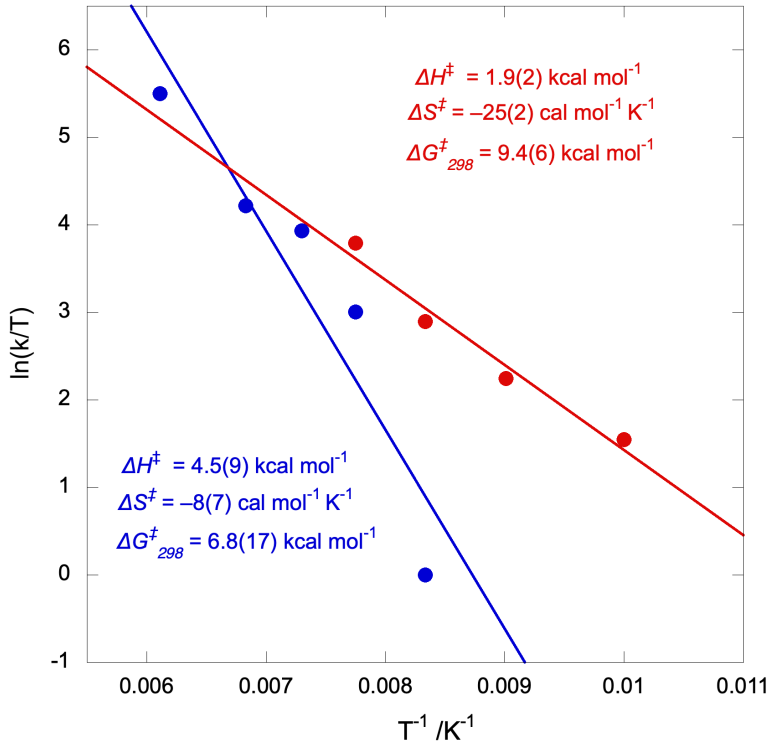

Figure S51. Eyring Plot for dynamics in $(Diso)_2Ru(PPh_3)$ (red circles) and $(Diso)_2Os(PPh_3)$ (blue circles).

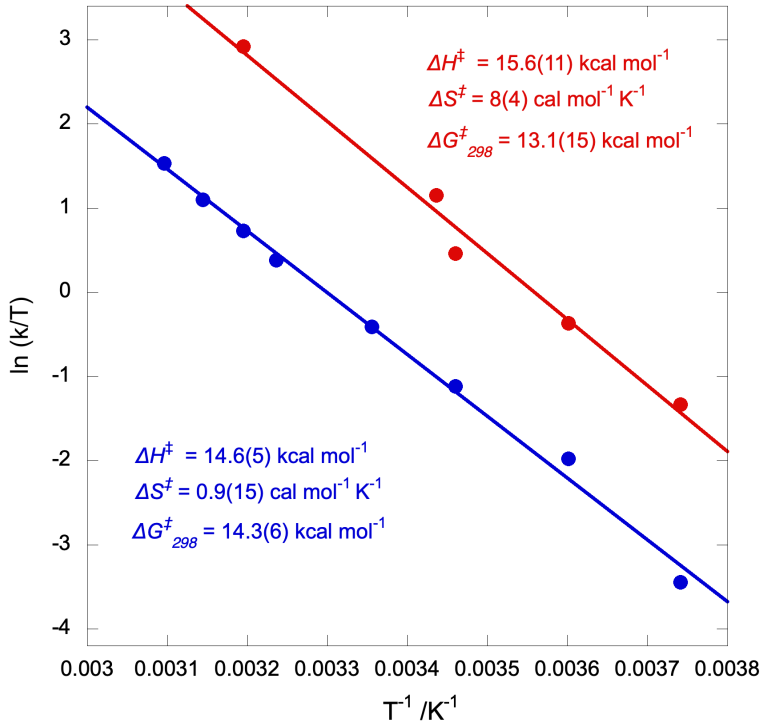

XI. Energies, average MOS values, and Cartesian Coordinates from DFT Calculations

Note: ap = 1,2-$C_6H_4(NH)O$

A. *cis*-α-$(ap)_2RuCl_2$ [N atoms mutually trans]

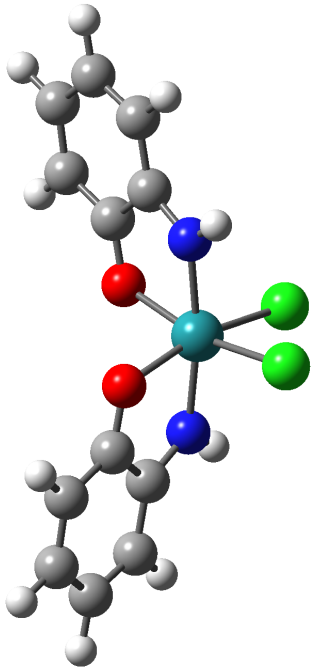

Energy of optimized structure = –1738.65314852 a.u.

MOS = –0.70(6)

Cartesian coordinates of optimized structure:

Center Number	Atomic Number	Coordinates (Angstroms) X	Y	Z
1	44	0.000000	0.000000	0.597342
2	17	-1.675248	0.139383	2.241549
3	8	1.513893	0.353044	-0.775836
4	7	0.000000	1.973027	0.442553
5	1	-0.682442	2.566213	0.918267
6	6	1.772402	1.590600	-0.984832
7	6	0.916031	2.563096	-0.315084
8	6	1.101701	3.962098	-0.536964
9	1	0.455280	4.676230	-0.034299
10	6	2.110337	4.365158	-1.370459
11	1	2.281234	5.422972	-1.544600
12	6	2.959378	3.410049	-2.022295
13	1	3.747177	3.778369	-2.673461
14	6	2.806216	2.057105	-1.847861
15	1	3.444974	1.331569	-2.339973

16	17	1.675248	-0.139383	2.241549
17	8	-1.513893	-0.353044	-0.775836
18	7	-0.000000	-1.973027	0.442553
19	1	0.682442	-2.566213	0.918267
20	6	-1.772402	-1.590600	-0.984832
21	6	-0.916031	-2.563096	-0.315084
22	6	-1.101701	-3.962098	-0.536964
23	1	-0.455280	-4.676230	-0.034299
24	6	-2.110337	-4.365158	-1.370459
25	1	-2.281234	-5.422972	-1.544600
26	6	-2.959378	-3.410049	-2.022295
27	1	-3.747177	-3.778369	-2.673461
28	6	-2.806216	-2.057105	-1.847861
29	1	-3.444974	-1.331569	-2.339973

B. ***cis*-α-(ap)$_2$OsCl$_2$ [N atoms mutually trans]**

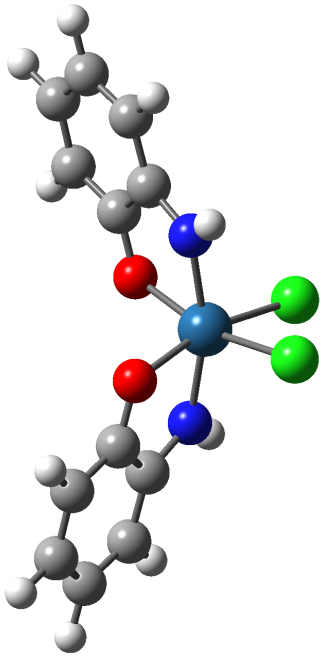

Energy of optimized structure = –1734.46454754 a.u.

MOS = –1.01(5)

Cartesian coordinates of optimized structure:

Center Number	Atomic Number	Coordinates (Angstroms) X	Y	Z
1	76	-0.000000	-0.000000	0.589042
2	17	0.743455	1.485007	2.267475
3	8	-0.234503	-1.568403	-0.717917
4	7	1.852606	-0.643368	0.313926

5	1	2.667832	-0.139690	0.667593
6	6	0.847230	-2.220525	-1.027104
7	6	2.075947	-1.708428	-0.476127
8	6	3.320156	-2.302230	-0.812949
9	1	4.241556	-1.902111	-0.398751
10	6	3.319548	-3.397782	-1.645587
11	1	4.256350	-3.881974	-1.903349
12	6	2.102039	-3.915386	-2.175668
13	1	2.143679	-4.781539	-2.829919
14	6	0.879860	-3.346511	-1.883669
15	1	-0.049879	-3.730918	-2.289171
16	17	-0.743455	-1.485007	2.267475
17	8	0.234503	1.568403	-0.717917
18	7	-1.852606	0.643368	0.313926
19	1	-2.667832	0.139690	0.667593
20	6	-0.847230	2.220525	-1.027104
21	6	-2.075947	1.708428	-0.476127
22	6	-3.320156	2.302230	-0.812949
23	1	-4.241556	1.902111	-0.398751
24	6	-3.319548	3.397782	-1.645587
25	1	-4.256350	3.881974	-1.903349
26	6	-2.102039	3.915386	-2.175668
27	1	-2.143679	4.781539	-2.829919
28	6	-0.879860	3.346511	-1.883669
29	1	0.049879	3.730918	-2.289171

C. *trans*-(ap)$_2$RuCl$_2$ (minimum-energy, C_s symmetry)

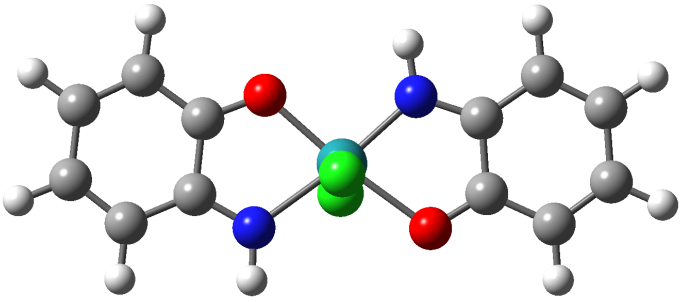

Energy of optimized structure = –1738.64451478 a.u.

avg. MOS = –0.64(6)

Cartesian coordinates of optimized structure:

Center Number	Atomic Number	Coordinates (Angstroms) X	Y	Z
1	44	0.054891	0.007832	0.000000
2	17	0.439012	-0.007824	2.329495
3	8	1.314640	1.709321	0.000000
4	7	-1.234057	1.447868	-0.000000
5	1	-2.245281	1.301918	-0.000000

6	6	0.649442	2.800588	0.000000
7	6	-0.807298	2.711965	-0.000000
8	6	-1.610616	3.890099	-0.000000
9	1	-2.694051	3.800371	-0.000000
10	6	-0.991045	5.111952	-0.000000
11	1	-1.580025	6.023681	-0.000000
12	6	0.439012	5.205933	-0.000000
13	1	0.891595	6.193947	-0.000000
14	6	1.247988	4.096574	0.000000
15	1	2.330307	4.168287	0.000000
16	17	0.439012	-0.007824	-2.329495
17	8	-1.279976	-1.468524	-0.000000
18	7	1.277392	-1.698987	0.000000
19	1	2.295295	-1.746113	0.000000
20	6	-0.833234	-2.671102	-0.000000
21	6	0.626384	-2.837099	0.000000
22	6	1.174025	-4.166164	0.000000
23	1	2.252559	-4.295843	0.000000
24	6	0.322827	-5.233716	0.000000
25	1	0.724083	-6.242950	0.000000
26	6	-1.106189	-5.062259	-0.000000
27	1	-1.735381	-5.947281	-0.000000
28	6	-1.679169	-3.818599	-0.000000
29	1	-2.754144	-3.672185	-0.000000

D. *trans*-(ap)$_2$RuCl$_2$ (constrained to C_2 symmetry)

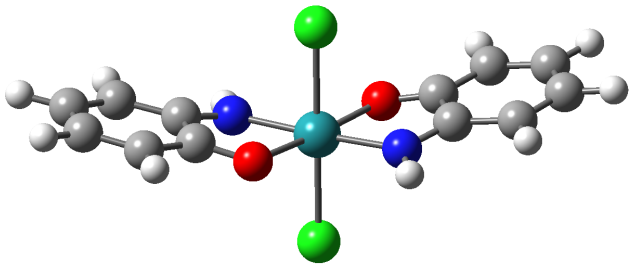

Energy of optimized structure = –1738.63629542 a.u.
*One imaginary frequency (278.0*i* cm^{-1})

MOS = –0.49(6)

Cartesian coordinates of optimized structure:

Center Number	Atomic Number	Coordinates (Angstroms) X	Y	Z
1	44	0.000000	0.000000	0.000000
2	17	0.000000	0.000000	2.408896
3	8	-2.064803	0.000000	-0.069604
4	7	-0.410458	-1.958519	-0.047710
5	1	0.250843	-2.719085	0.114471
6	6	-2.561641	-1.134851	-0.350720
7	6	-1.650162	-2.295774	-0.335764
8	6	-2.171662	-3.615950	-0.543354

9	1	-1.493790	-4.464954	-0.527046
10	6	-3.507579	-3.767750	-0.775340
11	1	-3.921335	-4.756869	-0.945631
12	6	-4.396705	-2.632970	-0.801094
13	1	-5.451695	-2.811084	-0.989378
14	6	-3.955523	-1.355754	-0.592293
15	1	-4.620986	-0.499361	-0.603858
16	17	0.000000	0.000000	-2.410412
17	8	2.064803	0.000000	-0.069604
18	7	0.410458	1.958519	-0.047710
19	1	-0.250843	2.719085	0.114471
20	6	2.561641	1.134851	-0.350720
21	6	1.650162	2.295774	-0.335764
22	6	2.171662	3.615950	-0.543354
23	1	1.493790	4.464954	-0.527046
24	6	3.507579	3.767750	-0.775340
25	1	3.921335	4.756869	-0.945631
26	6	4.396705	2.632970	-0.801094
27	1	5.451695	2.811084	-0.989378
28	6	3.955523	1.355754	-0.592293
29	1	4.620986	0.499361	-0.603858

E. *trans*-(ap)$_2$RuCl$_2$ (constrained to C_{2h} or C_i symmetry)

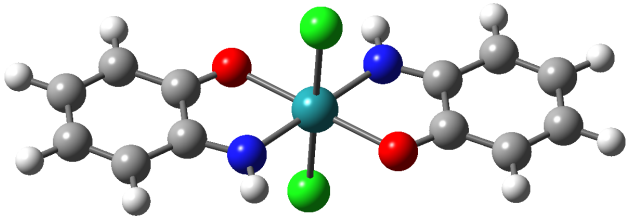

Energy of optimized structure = –1738.63511520 a.u.
*One imaginary frequency (52.3*i* cm^{-1})

MOS = –0.42(6)

Cartesian coordinates of optimized structure:

Center Number	Atomic Number	Coordinates (Angstroms) X	Y	Z
1	44	0.000000	0.000000	0.000000
2	17	-0.000000	0.000000	2.410937
3	8	1.076278	1.785888	-0.000000
4	7	-1.468001	1.367626	0.000000
5	1	-2.470680	1.172839	0.000000
6	6	0.350856	2.822126	0.000000
7	6	-1.117291	2.633661	0.000000
8	6	-1.984853	3.778155	0.000000
9	1	-3.061231	3.629205	0.000000
10	6	-1.432185	5.024266	0.000000

11	1	-2.069717	5.902988	0.000000
12	6	0.000000	5.209834	0.000000
13	1	0.385140	6.225699	0.000000
14	6	0.872181	4.158617	0.000000
15	1	1.948506	4.292546	0.000000
16	17	-0.000000	0.000000	-2.410937
17	8	-1.076278	-1.785888	-0.000000
18	7	1.468001	-1.367626	0.000000
19	1	2.470680	-1.172839	0.000000
20	6	-0.350856	-2.822126	0.000000
21	6	1.117291	-2.633661	0.000000
22	6	1.984853	-3.778155	0.000000
23	1	3.061231	-3.629205	0.000000
24	6	1.432185	-5.024266	0.000000
25	1	2.069717	-5.902988	0.000000
26	6	-0.000000	-5.209834	0.000000
27	1	-0.385140	-6.225699	0.000000
28	6	-0.872181	-4.158617	0.000000
29	1	-1.948506	-4.292546	0.000000

F. ***trans*-(ap)$_2$OsCl$_2$ (minimum-energy, C_s symmetry)**

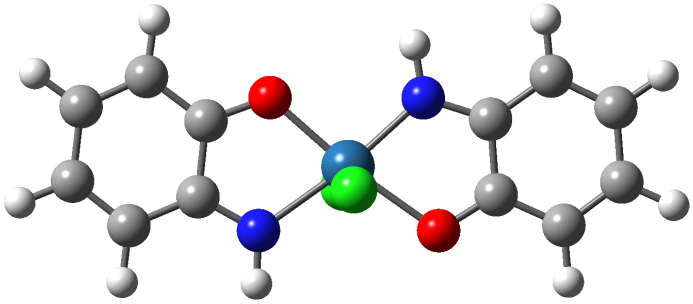

Energy of optimized structure = –1734.45102859 a.u.

avg. MOS = –0.90(6)

Cartesian coordinates of optimized structure:

Center Number	Atomic Number	Coordinates (Angstroms) X	Y	Z
1	76	0.052996	0.000672	0.000000
2	17	0.473535	0.005608	2.318048
3	8	1.316381	1.701183	0.000000
4	7	-1.223422	1.466272	-0.000000
5	1	-2.235653	1.329735	-0.000000
6	6	0.658636	2.815176	-0.000000
7	6	-0.785536	2.743006	-0.000000
8	6	-1.578848	3.918734	-0.000000
9	1	-2.663131	3.837590	-0.000000
10	6	-0.949343	5.141914	-0.000000
11	1	-1.532916	6.057026	-0.000000

12	6	0.473535	5.219544	-0.000000
13	1	0.941101	6.200575	-0.000000
14	6	1.271656	4.094502	-0.000000
15	1	2.354684	4.155794	0.000000
16	17	0.473535	0.005608	-2.318048
17	8	-1.297720	-1.456916	-0.000000
18	7	1.232729	-1.736947	0.000000
19	1	2.248530	-1.799450	0.000000
20	6	-0.882004	-2.689674	0.000000
21	6	0.559354	-2.876981	0.000000
22	6	1.079858	-4.208317	0.000000
23	1	2.155266	-4.362083	0.000000
24	6	0.204236	-5.264079	0.000000
25	1	0.590033	-6.279514	0.000000
26	6	-1.213524	-5.067785	0.000000
27	1	-1.864058	-5.936965	0.000000
28	6	-1.756146	-3.804704	-0.000000
29	1	-2.827395	-3.631907	-0.000000

G. *trans*-(ap)$_2$OsCl$_2$ (constrained to C_2 symmetry)

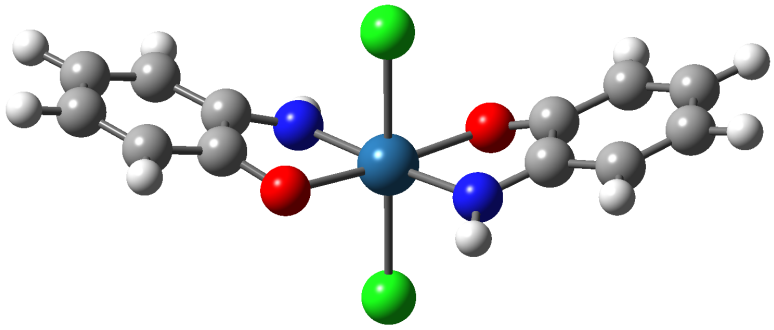

Energy of optimized structure = –1734.43812416 a.u.

avg. MOS = –0.73(6)

Cartesian coordinates of optimized structure:

Center Number	Atomic Number	Coordinates (Angstroms) X	Y	Z
1	76	0.000000	0.000000	0.314431
2	17	0.000000	0.000000	2.735336
3	8	1.033860	1.768954	0.216376
4	7	-1.466200	1.368786	0.255994
5	1	-2.437059	1.221948	0.530507
6	6	0.326713	2.760842	-0.198901
7	6	-1.125214	2.582146	-0.169629
8	6	-1.984857	3.682647	-0.464588
9	1	-3.062046	3.544074	-0.436035
10	6	-1.423803	4.884243	-0.805628
11	1	-2.059517	5.729667	-1.049994
12	6	-0.000000	5.053594	-0.849502

13	1	0.397736	6.026437	-1.124005
14	6	0.864245	4.031025	-0.548418
15	1	1.941498	4.155523	-0.568231
16	17	-0.000000	-0.000000	-2.100464
17	8	-1.033860	-1.768954	0.216376
18	7	1.466200	-1.368786	0.255994
19	1	2.437059	-1.221948	0.530507
20	6	-0.326713	-2.760842	-0.198901
21	6	1.125214	-2.582146	-0.169629
22	6	1.984857	-3.682647	-0.464588
23	1	3.062046	-3.544074	-0.436035
24	6	1.423803	-4.884243	-0.805628
25	1	2.059517	-5.729667	-1.049994
26	6	-0.000000	-5.053594	-0.849502
27	1	-0.397736	-6.026437	-1.124005
28	6	-0.864245	-4.031025	-0.548418
29	1	-1.941498	-4.155523	-0.568231

H. *trans*-$(ap)_2OsCl_2$ (constrained to C_{2h} symmetry)

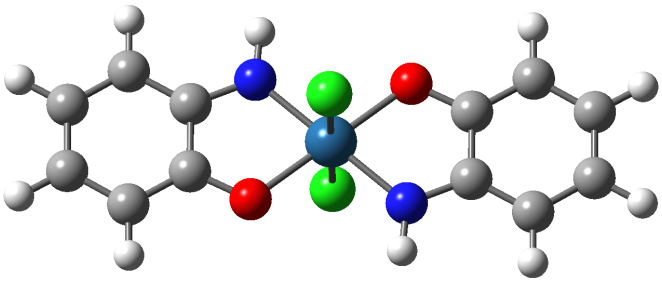

Energy of optimized structure = –1734.42952511 a.u.

MOS = –1.51(9)

Cartesian coordinates of optimized structure:

Center Number	Atomic Number	Coordinates (Angstroms) X	Y	Z
1	76	0.000000	0.000000	0.000000
2	17	-0.000000	-0.000000	2.366569
3	8	1.031835	1.704196	-0.000000
4	7	-1.484769	1.321945	-0.000000
5	1	-2.481205	1.115521	0.000000
6	6	0.297497	2.816656	-0.000000
7	6	-1.121744	2.639522	-0.000000
8	6	-1.963263	3.762169	-0.000000
9	1	-3.042321	3.632489	-0.000000
10	6	-1.394196	5.036274	-0.000000
11	1	-2.039842	5.909301	-0.000000
12	6	0.000000	5.203732	-0.000000
13	1	0.420205	6.204891	-0.000000
14	6	0.854161	4.098597	-0.000000

15	1	1.933711	4.208490	-0.000000
16	17	-0.000000	-0.000000	-2.366569
17	8	-1.031835	-1.704196	-0.000000
18	7	1.484769	-1.321945	-0.000000
19	1	2.481205	-1.115521	0.000000
20	6	-0.297497	-2.816656	-0.000000
21	6	1.121744	-2.639522	-0.000000
22	6	1.963263	-3.762169	-0.000000
23	1	3.042321	-3.632489	-0.000000
24	6	1.394196	-5.036274	-0.000000
25	1	2.039842	-5.909301	-0.000000
26	6	-0.000000	-5.203732	-0.000000
27	1	-0.420205	-6.204891	-0.000000
28	6	-0.854161	-4.098597	-0.000000
29	1	-1.933711	-4.208490	-0.000000

I. $(ap)_2Ru(PMe_3)$

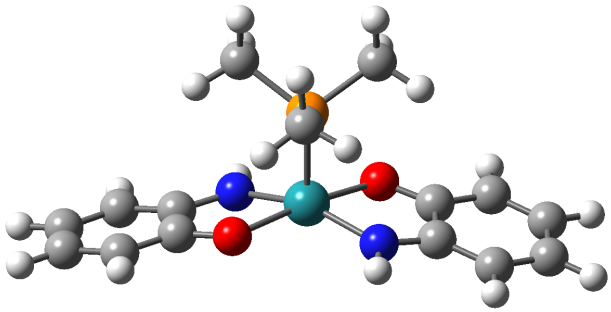

Energy of optimized structure = –1279.35386162 a.u.

avg. MOS = –1.27(5)

Cartesian coordinates of optimized structure:

Center Number	Atomic Number	Coordinates (Angstroms) X	Y	Z
1	44	0.011386	-0.275944	0.005788
2	8	-1.608380	-0.161238	1.310756
3	7	-1.455268	-0.863742	-1.150265
4	1	-1.367852	-1.215265	-2.104349
5	6	-2.748364	-0.511410	0.759500
6	6	-2.710216	-0.942784	-0.608736
7	6	-3.886909	-1.385062	-1.250295
8	6	-5.086609	-1.375640	-0.557095
9	1	-5.997755	-1.709672	-1.045096
10	6	-5.131296	-0.932174	0.783702
11	6	-3.986276	-0.502575	1.439005
12	1	-4.012423	-0.174742	2.474355
13	15	-0.025307	1.971504	-0.199888
14	6	-1.448028	2.614367	-1.177098
15	1	-1.463715	3.710165	-1.171062

16	1	-1.371008	2.255116	-2.206933
17	1	-2.380984	2.235066	-0.750220
18	6	1.455527	2.699795	-1.013961
19	1	1.388893	3.793081	-1.048734
20	1	2.354315	2.407776	-0.462748
21	1	1.539144	2.301773	-2.028908
22	6	-0.159515	2.873953	1.401622
23	1	-0.276662	3.952357	1.244867
24	1	-1.019764	2.480887	1.950061
25	1	0.740823	2.690366	1.995266
26	1	-3.840186	-1.723448	-2.283769
27	1	-6.080774	-0.934096	1.312940
28	8	1.599059	-0.667548	-1.256667
29	7	1.504140	-0.367601	1.284012
30	1	1.444874	-0.308840	2.301146
31	6	2.752535	-0.780652	-0.641565
32	6	2.748971	-0.637195	0.787231
33	6	3.946495	-0.782368	1.521902
34	6	5.128744	-1.046930	0.851124
35	1	6.054929	-1.157726	1.407766
36	6	5.137866	-1.174868	-0.557111
37	6	3.974266	-1.043894	-1.299852
38	1	3.973101	-1.151324	-2.380735
39	1	3.927190	-0.684342	2.605828
40	1	6.075772	-1.383865	-1.065219

J. $(ap)_2Ru(PMe_3)$ (with $(ap)_2Ru(P)$ fragment constrained to C_2 symmetry)

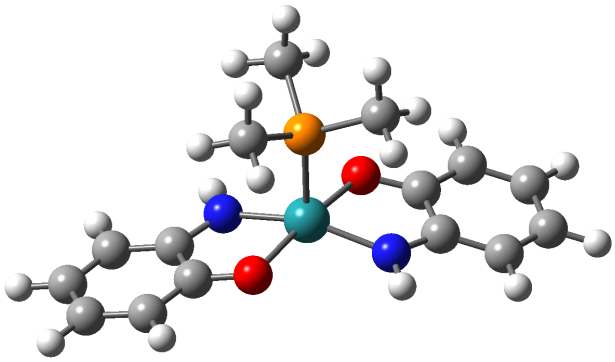

Energy of optimized structure = –1279.35345260 a.u.

MOS = –1.27(5)

Cartesian coordinates of optimized structure:

Center Number	Atomic Number	Coordinates (Angstroms) X	Y	Z
1	44	0.001653	-0.268797	-0.000400
2	15	0.000392	1.990368	-0.007834
3	6	1.474149	2.764723	-0.791196
4	1	1.420961	3.857600	-0.731387
5	1	1.530882	2.450872	-1.836726

6	1	2.380379	2.415954	-0.287491
7	6	-0.073929	2.753420	1.669565
8	1	-0.144811	3.845727	1.609946
9	1	0.824415	2.478557	2.229919
10	1	-0.943693	2.354615	2.199203
11	6	-1.432357	2.749479	-0.882689
12	1	-1.422936	3.839853	-0.773379
13	1	-2.363429	2.350413	-0.470067
14	1	-1.388230	2.488253	-1.943536
15	8	1.604953	-0.415562	-1.308678
16	7	1.479781	-0.616532	1.242448
17	1	1.405520	-0.766230	2.249260
18	6	2.750427	-0.651826	-0.713257
19	6	2.728991	-0.797337	0.715034
20	6	3.914810	-1.099218	1.419436
21	1	3.881074	-1.221126	2.500553
22	6	5.105417	-1.231733	0.724111
23	1	6.023163	-1.459997	1.258506
24	6	5.133203	-1.071296	-0.680094
25	1	6.076664	-1.180916	-1.208710
26	6	3.980262	-0.783698	-1.395421
27	1	3.993494	-0.672069	-2.475848
28	8	-1.601487	-0.408738	1.308821
29	7	-1.476081	-0.626353	-1.240927
30	1	-1.401649	-0.782591	-2.246732
31	6	-2.746694	-0.650194	0.714973
32	6	-2.725090	-0.805077	-0.712330
33	6	-3.910569	-1.112911	-1.414725
34	1	-3.876693	-1.241893	-2.495017
35	6	-5.101030	-1.242176	-0.718539
36	1	-6.018519	-1.474976	-1.251417
37	6	-5.129000	-1.072532	0.684580
38	1	-6.072340	-1.179725	1.213910
39	6	-3.976384	-0.778946	1.397994
40	1	-3.989744	-0.660224	2.477663

K. $(ap)_2Os(PMe_3)$ (with $(ap)_2Os(P)$ fragment constrained to C_2 symmetry)

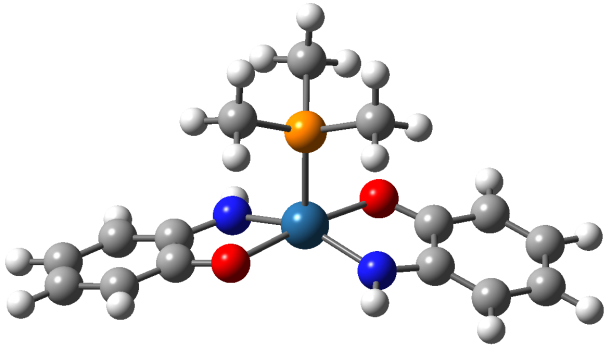

Energy of optimized structure = –1275.15251466 a.u.
*One imaginary frequency (1.7*i* cm^{-1})

avg. MOS = –1.40(6)

Cartesian coordinates of optimized structure:

Center Number	Atomic Number	Coordinates (Angstroms) X	Y	Z
1	76	0.002113	-0.173787	0.000309
2	15	0.000532	2.103279	-0.005728
3	6	1.484292	2.877100	-0.770726
4	1	1.420614	3.970279	-0.729309
5	1	1.564843	2.545080	-1.808892
6	1	2.381875	2.544787	-0.241127
7	6	-0.105914	2.885268	1.662319
8	1	-0.173774	3.977080	1.589404
9	1	0.781157	2.615113	2.242626
10	1	-0.986552	2.492474	2.178211
11	6	-1.427541	2.834123	-0.911761
12	1	-1.427129	3.925882	-0.816952
13	1	-2.359435	2.433131	-0.503248
14	1	-1.365589	2.556935	-1.967354
15	8	1.639780	-0.318889	-1.300277
16	7	1.472410	-0.608189	1.231259
17	1	1.374250	-0.812724	2.226519
18	6	2.774184	-0.627930	-0.703952
19	6	2.729863	-0.828105	0.710250
20	6	3.885062	-1.209439	1.418012
21	1	3.830449	-1.372214	2.492945
22	6	5.081415	-1.364822	0.732447
23	1	5.980744	-1.652744	1.269294
24	6	5.134081	-1.150342	-0.661206
25	1	6.078532	-1.278683	-1.183971
26	6	4.002095	-0.786095	-1.378613
27	1	4.034457	-0.633030	-2.453552
28	8	-1.635357	-0.314265	1.301652
29	7	-1.467576	-0.616751	-1.228315
30	1	-1.369129	-0.826423	-2.222477
31	6	-2.769328	-0.628037	0.706978
32	6	-2.724724	-0.835646	-0.706143
33	6	-3.879390	-1.222331	-1.411869
34	1	-3.824547	-1.390728	-2.485924
35	6	-5.075528	-1.375738	-0.725485
36	1	-5.974455	-1.667751	-1.260794
37	6	-5.128498	-1.153944	0.667011
38	1	-6.072771	-1.280822	1.190453
39	6	-3.997021	-0.784328	1.382473
40	1	-4.029600	-0.625610	2.456585

References

S1 J. S. Siegel and F. A. L. Anet, *J. Org. Chem.*, 1988, **53**, 2629-2630.

S2 A. J. Godó, A. C. Bényei, B. Duff, D. A. Egan and P. Buglyó, *RSC Adv.*, 2012, **2**, 1486-1495.

S3 G. A. Abakumov, N. O. Druzhkov, Y. A. Kurskii and A. S. Shavyrin, *Russ. Chem. Bull.*, 2003**, 52**, 712-717.

S4 T. B. Ditri, A. E. Carpenter, D. S. Ripatti, C. E. Moore, A. L. Rheingold and J. S. Figueroa, *Inorg. Chem.*, 2013, **52**, 13216-13229.

S5 N. G. Connelly and W. E. Geiger, *Chem. Rev.*, 1996, **96**, 877-910.

S6 D. Lionetti, A. J. Medvecz, V. Ugrinova, M. Quiroz-Guzman, B. C. Noll and S. N. Brown, *Inorg. Chem.*, 2010, **49**, 4687-4697.

S7 A. J. Gordon and R. A. Ford, *The Chemist's Companion*, John Wiley and Sons: New York, 1972, p. 303.

S8 W. H. Sikorski, A. W. Sanders and H. J. Reich, *Magn. Reson. Chem.*, 1998, **36**, S118-2124.

S9 M. J. Frisch, G. W. Trucks, H. B. Schlegel, G. E. Scuseria, M. A. Robb, J. R. Cheeseman, G. Scalmani, V. Barone, G. A. Petersson, H. Nakatsuji, X. Li, M. Caricato, A. V. Marenich, J. Bloino, B. G. Janesko, R. Gomperts, B. Mennucci, H. P. Hratchian, J. V. Ortiz, A. F. Izmaylov, J. L. Sonnenberg, D. Williams-Young, F. Ding, F. Lipparini, F. Egidi, J. Goings, B. Peng, A. Petrone, T. Henderson, D. Ranasinghe, V. G. Zakrzewski, J. Gao, N. Rega, G. Zheng, W. Liang, M. Hada, M. Ehara, K. Toyota, R. Fukuda, J. Hasegawa, M. Ishida, T. Nakajima, Y. Honda, O. Kitao, H. Nakai, T. Vreven, K. Throssell, J. A. Montgomery Jr., J. E. Peralta, F. Ogliaro, M. J. Bearpark, J. J. Heyd, E.

N. Brothers, K. N. Kudin, V. N. Staroverov, T. A. Keith, R. Kobayashi, J. Normand, K. Raghavachari, A. P. Rendell, J. C. Burant, S. S. Iyengar, J. Tomasi, M. Cossi, J. M. Millam, M. Klene, C. Adamo, R. Cammi, J. W. Ochterski, R. L. Martin, K. Morokuma, O. Farkas, J. B. Foresman and D. J. Fox, *Gaussian 16, Revision B.01*, Gaussian, Inc., Wallingford CT, 2016.

S10 A. N. Erickson, J. Gianino, S. J. Markovitz and S. N. Brown, *Inorg. Chem.*, 2021, **60**, 4004-4014.

S11 P. van der Sluis and A. L. Spek, *Acta Cryst.*, 1990, **A46**, 194-201.

S12 G. M. Sheldrick, *Acta Cryst. A*, 2008, **A64**, 112-122.

S13 A. J. C. Wilson, *International Tables for Crystallography*, Kluwer Academic Publishers, Dordrecht, The Netherlands, 1992, vol. C.

S14 S. N. Brown, *Inorg. Chem.*, 2012, **51**, 1251-1260.